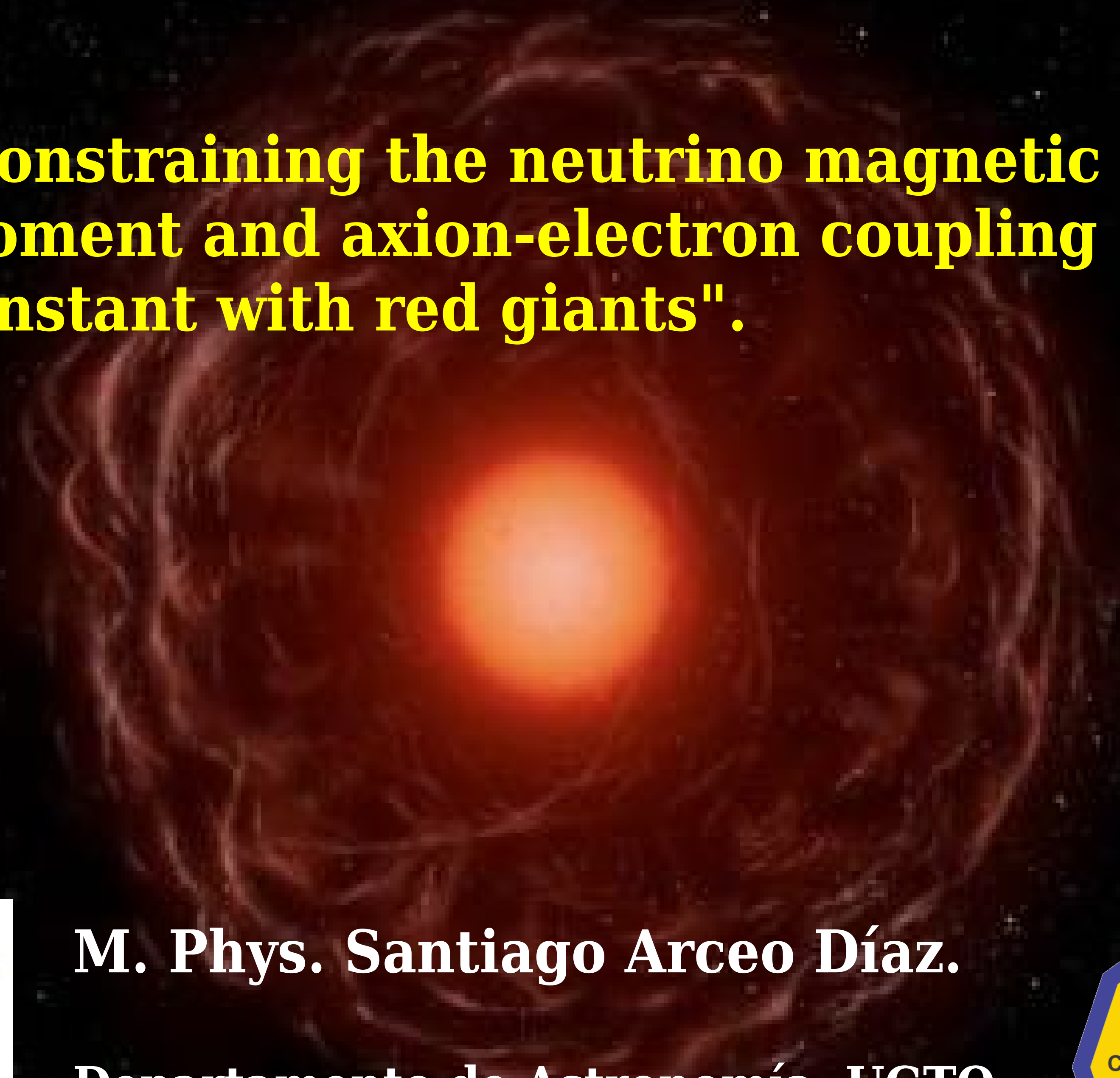

"Constraining the neutrino magnetic dipole moment and axion-electron coupling constant with red giants".

M. Phys. Santiago Arceo Díaz.

Departamento de Astronomía, UGTO.
Instituto Tecnológico de Colima.

Objective of the project

To establish a maximum constrain on the magnetic dipole moment of neutrinos.

Motivation:
Stellar modeling simulations provide a limit at least one order of magnitude larger than the one suggested by experimental data.

Tools

Simulation: Eggleton code (STARS) for constructing stellar tracks from main-sequence to the tip-RGB.

Theory: Energy loss prescriptions for neutrino cooling (Itoh et al., 1992, Haft et al.,1994, Kantor 2007).

Modifications on energy losses due a non-zero magnetic dipole moment of neutrinos (Raffelt et al, 1992) and the axion-electron coupling constant (Raffelt, 1995).

Observations: luminosity of the tip-RGB from the database by Valenti, Ferraro & Origlia (Valenti et al., 2006)

In Short:

Learn how to use and update some parts of Eggleton's code.

Learn the basics about neutrinos in stellar astrophysics.

Find out everything I could

Standard Model of Particle Physics

To the most fundamental level, all known matter in the Universe is made of twelve types or particles

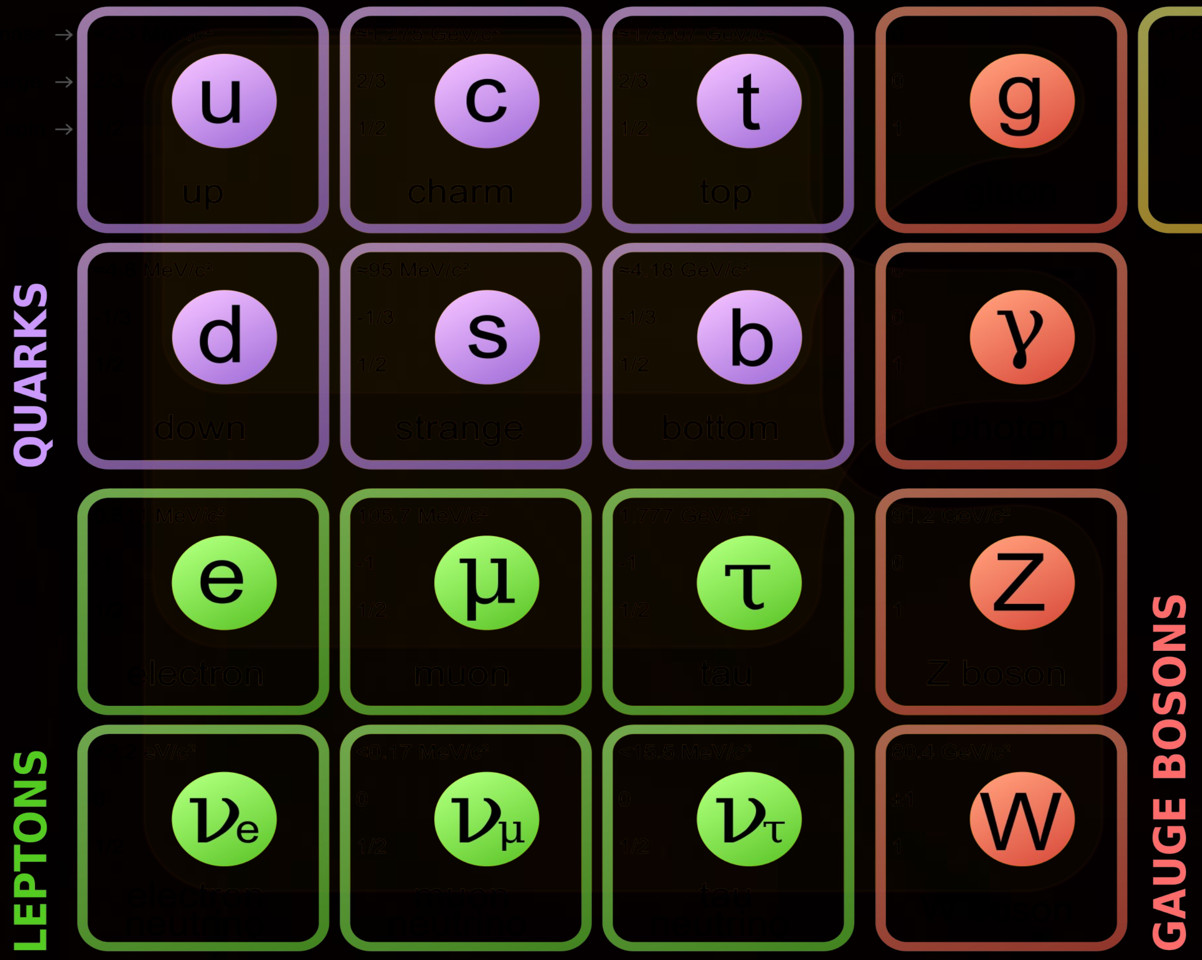

Interacting through three fundamental forces

+

Gravity

Physics out of the standard model:

Exotic matter

Unknown properties for know matter

Unknown interactions

Neutrinos, are the lightest known massive particles and the less interacting

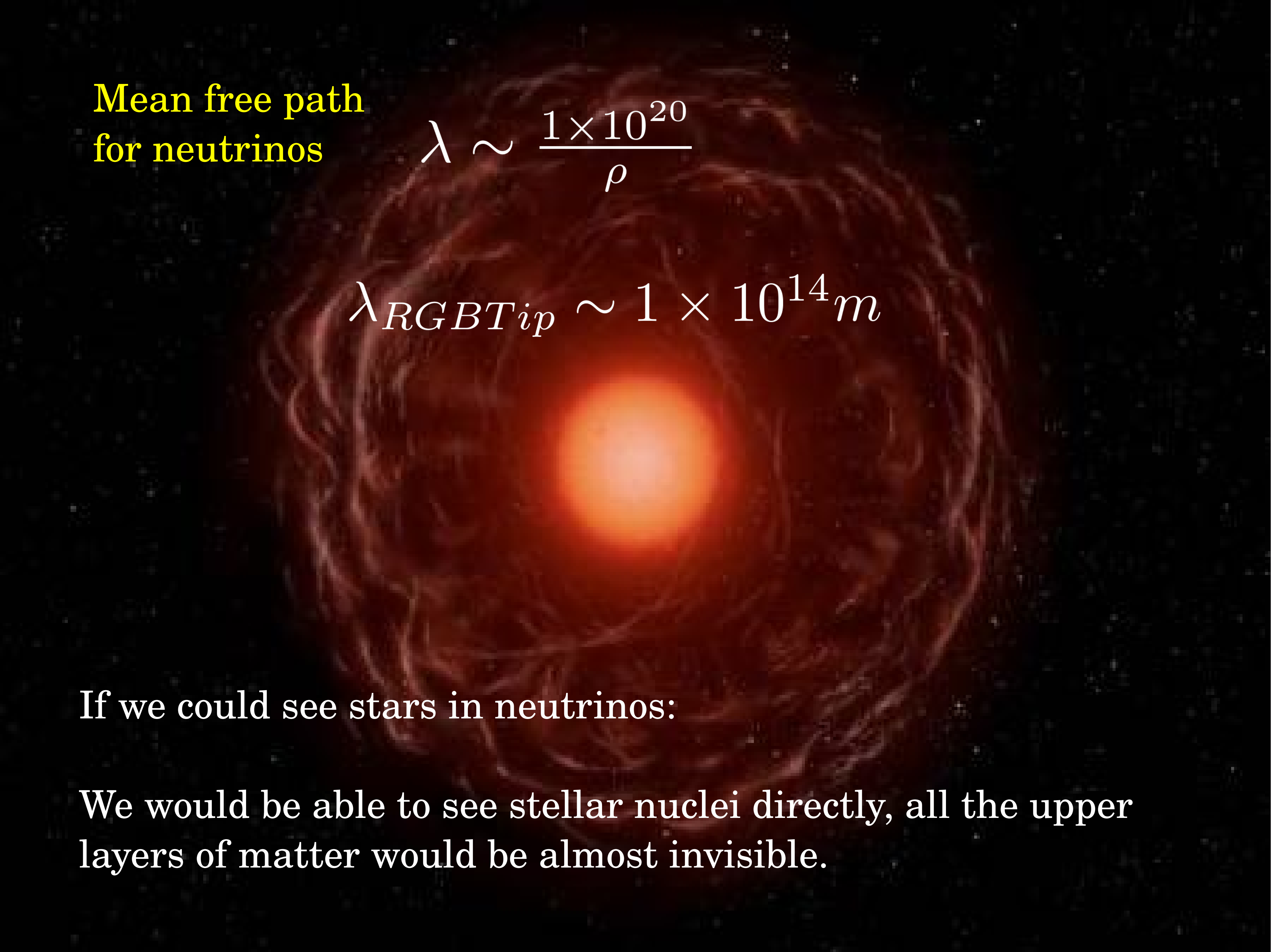

Mean free path
for neutrinos

$$\lambda \sim \frac{1\times10^{20}}{\rho}$$

$$\lambda_{RGBTip} \sim 1 \times 10^{14} m$$

If we could see stars in neutrinos:

We would be able to see stellar nuclei directly, all the upper layers of matter would be almost invisible.

Neutrinos: Ghost Particles

The most efficient known energy burglars.

Why to use low mass stars to constraint fundamental particles?

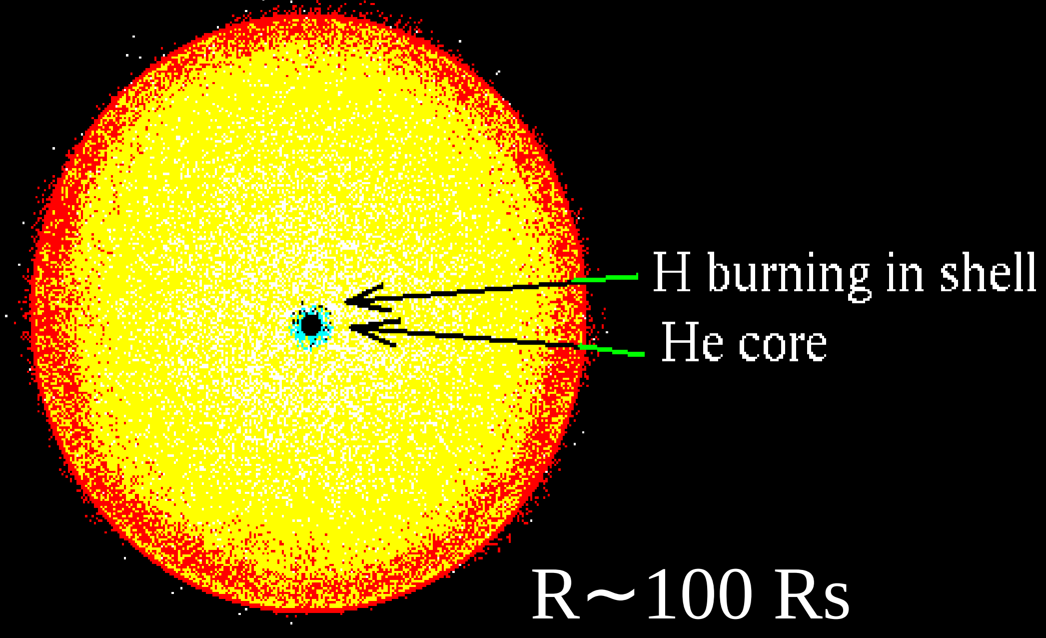

R~100 Rs

Low mass stars evolve into Red giants

Surface Luminosity depends strongly on the mass of the degenerate helium core (which has almost an universal value)

The luminosity on the tip-RGB controlled by the amount of energy losses (as neutrino or axion production)

- ρ~1x104 -1x106 g/cm3
- Tc~1x107-1x108 K

Mc=Mc(Lv)

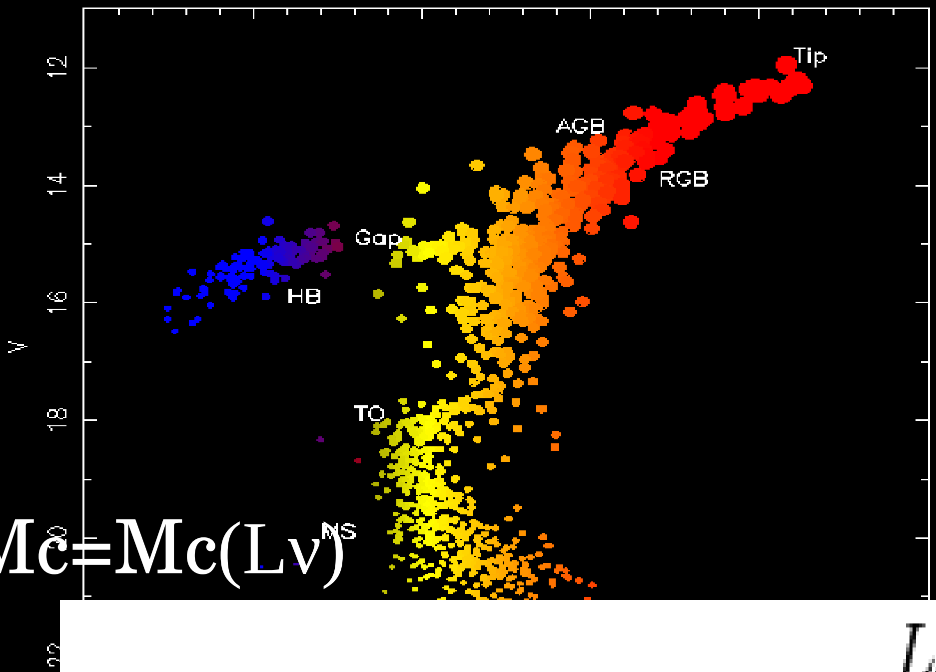

$$M_{bol_{star}} - M_{bol_{Sun}} = -2.5 \log_{10} \frac{L_{star}}{L_{\odot}}$$

Helium luminosity as a clock during the RGB

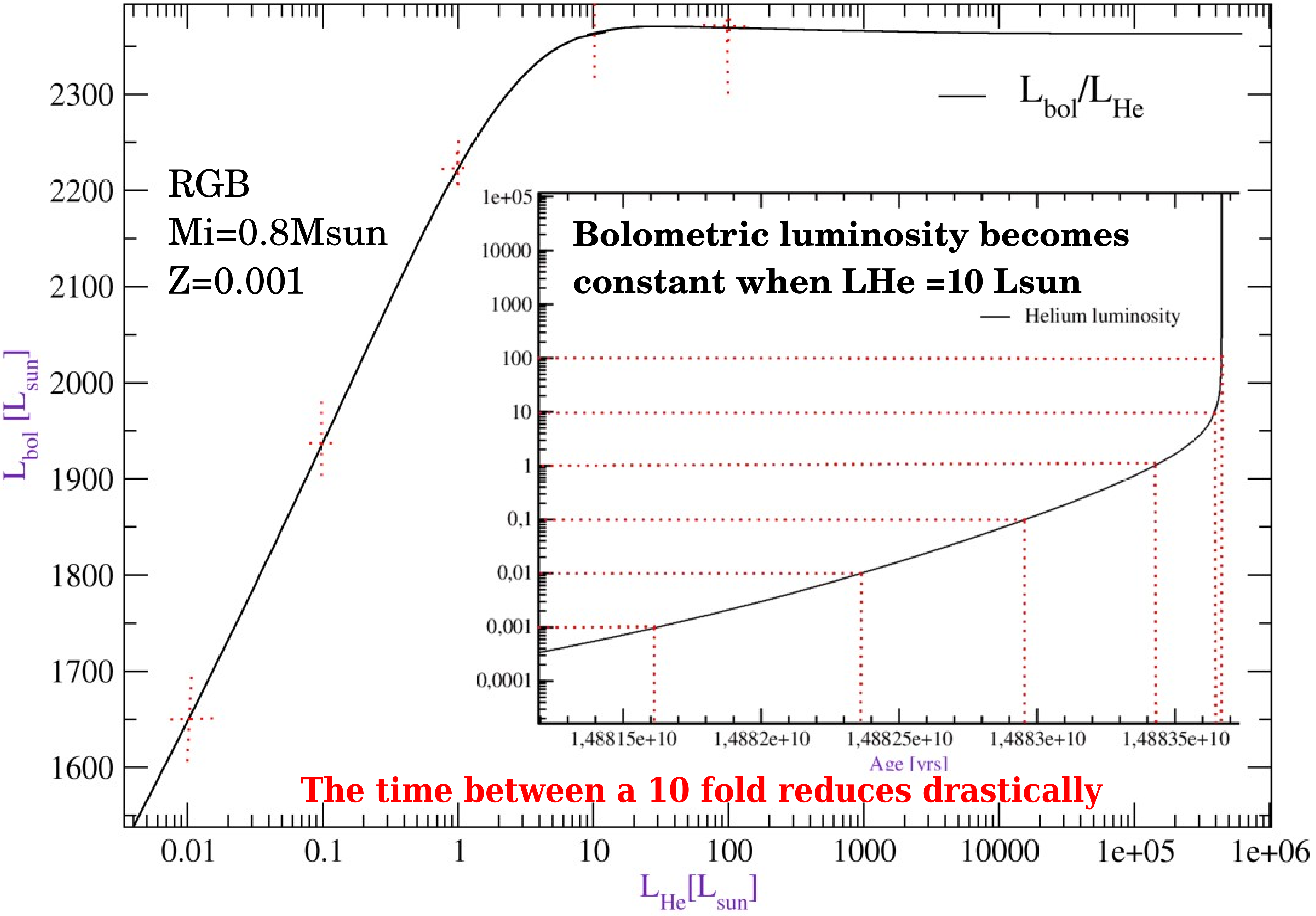

Bolometric luminosity becomes constant when LHe =10 Lsun

The time between a 10 fold reduces drastically

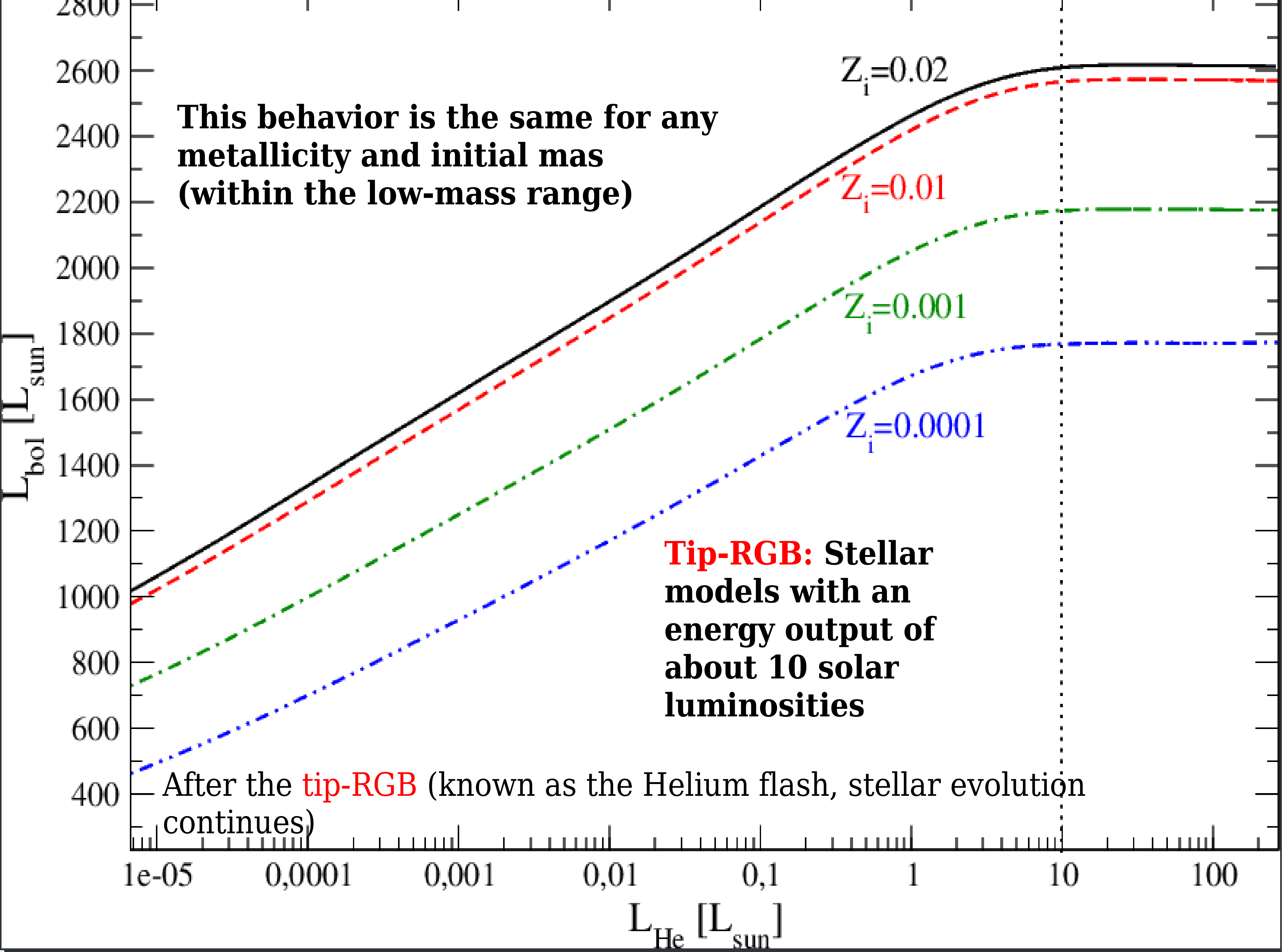

This behavior is the same for any metallicity and initial mas (within the low-mass range)

Tip-RGB: Stellar models with an energy output of about 10 solar luminosities

After the tip-RGB (known as the Helium flash, stellar evolution continues)

Thermal neutrino processes

Apart from nuclear reactions, neutrinos can also be produced by reactions involving electrons losing some of their energy

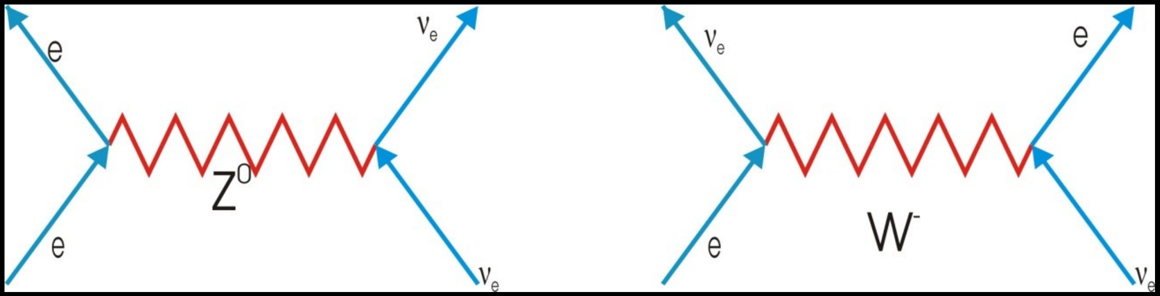

On a high density environment, composed by plasma, low energy neutrinos are produced mostly by:

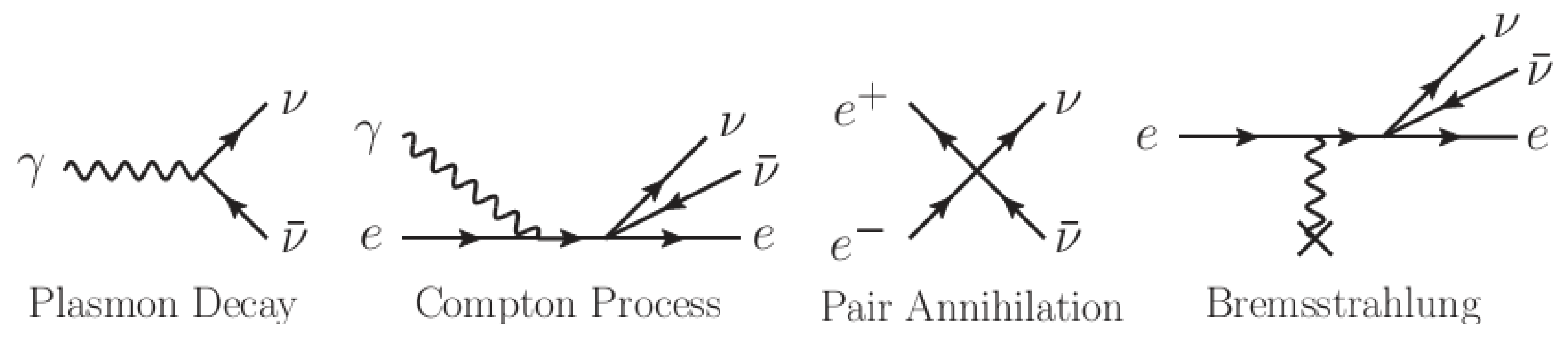

These processes are the ones producing neutrinos inside the He core of red giants

If neutrinos do have a non-zero magnetic dipole moment, they can be produced also by photons

i.e. all processes involving photons losing would be able to produce neutrino-antineutrino pairs.

Parameterized neutrino magnetic dipole moment:
(Raffelt & Haft, 1990)

$$\mu_{12} = \frac{\mu_\nu}{10^{-2}\mu_B}$$

Current experimental limit
Beda et al., 2013

$$\mu_\nu < 3 \times 10^{-11} \mu_B$$

We propose the limit:

$$\mu_\nu \simeq 2.2 \times 10^{-12} \mu_B$$

Stellar evolution code

Eggleton code (1973): **Adaptive non – Lagrangian mesh with 199 control points.**

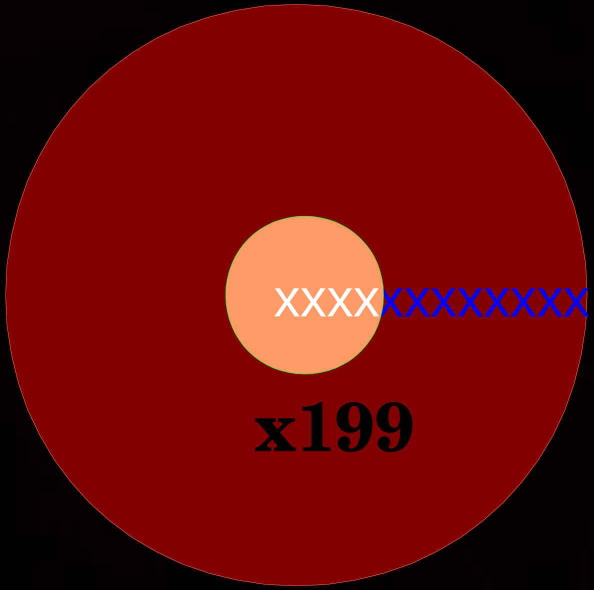

r = 0 → photosphere, optical thickness= 2/3

Solve structure and composition equations by using 11 independent variables

ln f
ln T
X16
ln m
X1
C
ln r
L
X4
X12
X20

Nuclear reaction rates: OPAL 96, Chen & Tout, 2006.

Non-dust driven mass- loss: Schröder, 2005.

Electron opacities: Itoh, 1984.

Neutrino production: For plasmon decay, you can select between Kantor et al., 2007, Haft et al., 1994, Itoh et al., 1992. For the other processes Itoh et al., 1992.

Effects of neutrino cooling in low-mass stars

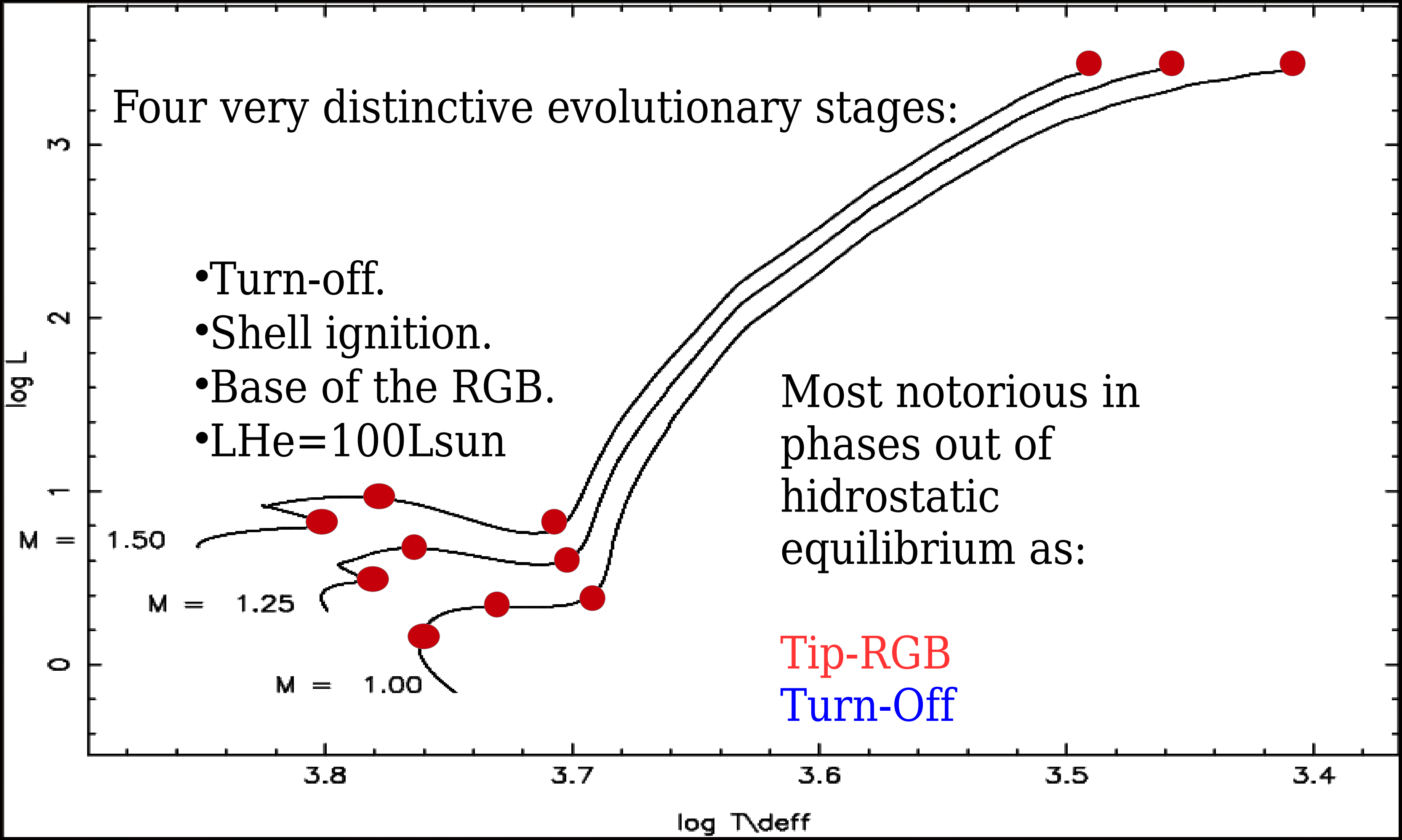

Four very distinctive evolutionary stages:

- Turn-off.
- Shell ignition.
- Base of the RGB.
- LHe=100Lsun

Most notorious in phases out of hidrostatic equilibrium as:

Tip-RGB
Turn-Off

Stellar evolution depends on several factors as initial mass, chemical composition, mixing length theory… but among others on the balance between energy production and depletion

Neutrino emission is one of the major factors of energy depletion

Neutrino production from main sequence to the tip-RGB

Neutrino luminosity VS radial distance
(The Sun nowadays, more or less)

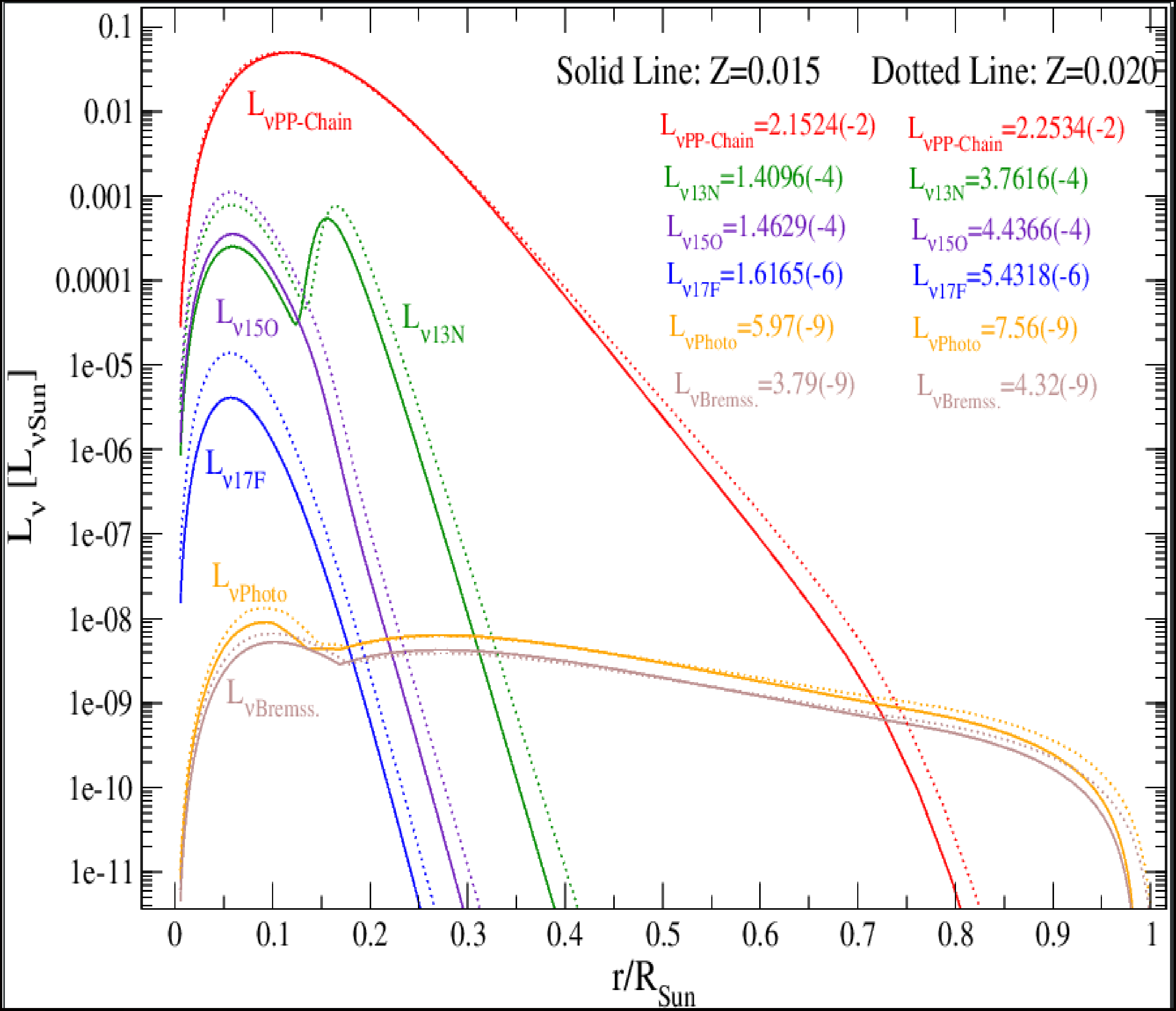

Neutrinos are mostly produced by nuclear reactions (involving mostly the PP-Chain and little from the CNO process)

There is an slight dependence on metallicity, affecting mostly the CNO cycle.

Thermal reactions are still too weak

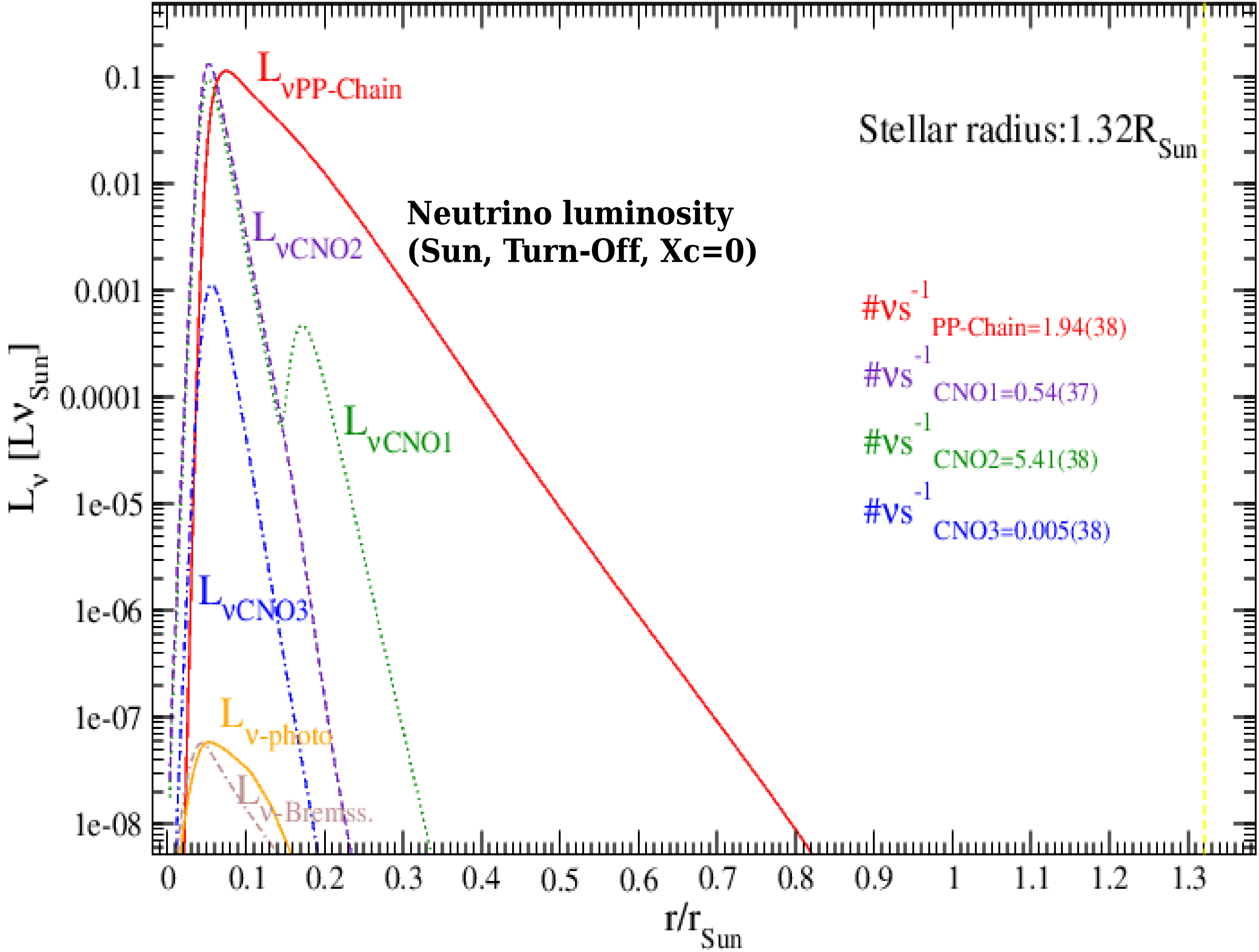
$L_{\nu PP\text{-}Chain}$
Stellar radius:1.32R_{Sun}
Neutrino luminosity
(Sun, Turn-Off, Xc=0)
$L_{\nu CNO2}$
$L_{\nu CNO1}$
$L_{\nu CNO3}$
$L_{\nu\text{-}photo}$
$L_{\nu\text{-}Bremss.}$
$\#\nu s^{-1}_{PP\text{-}Chain}$=1.94(38)
$\#\nu s^{-1}_{CNO1}$=0.54(37)
$\#\nu s^{-1}_{CNO2}$=5.41(38)
$\#\nu s^{-1}_{CNO3}$=0.005(38)
L_ν [$L\nu_{Sun}$]
0.1
0.01
0.001
0.0001
1e-05
1e-06
1e-07
1e-08
0
0.1
0.2
0.3
0.4
0.5
0.6
0.7
0.8
0.9
1
1.1
1.2
1.3
r/r_{Sun}

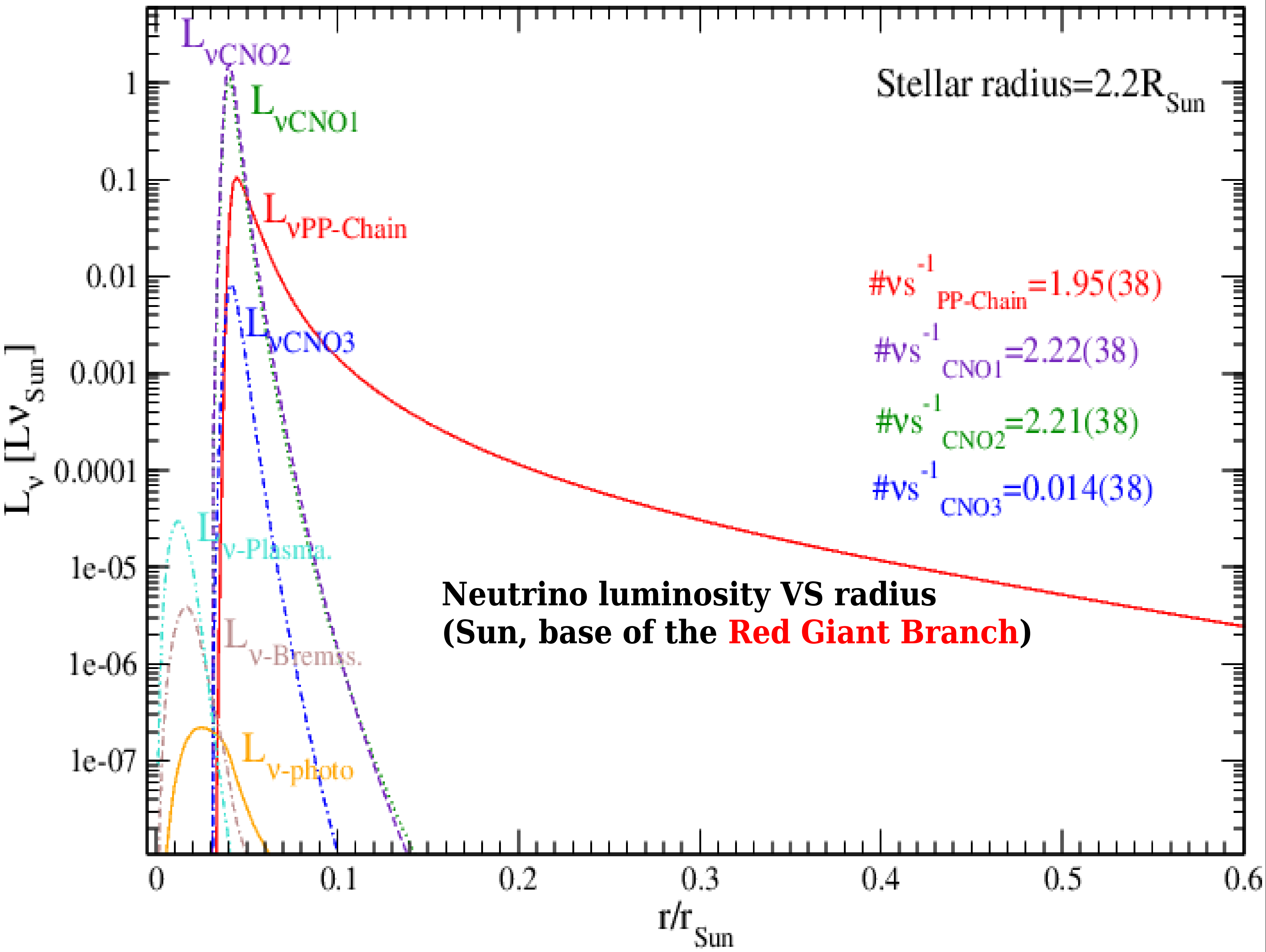

Neutrino luminosity VS radius
(Sun, base of the Red Giant Branch)

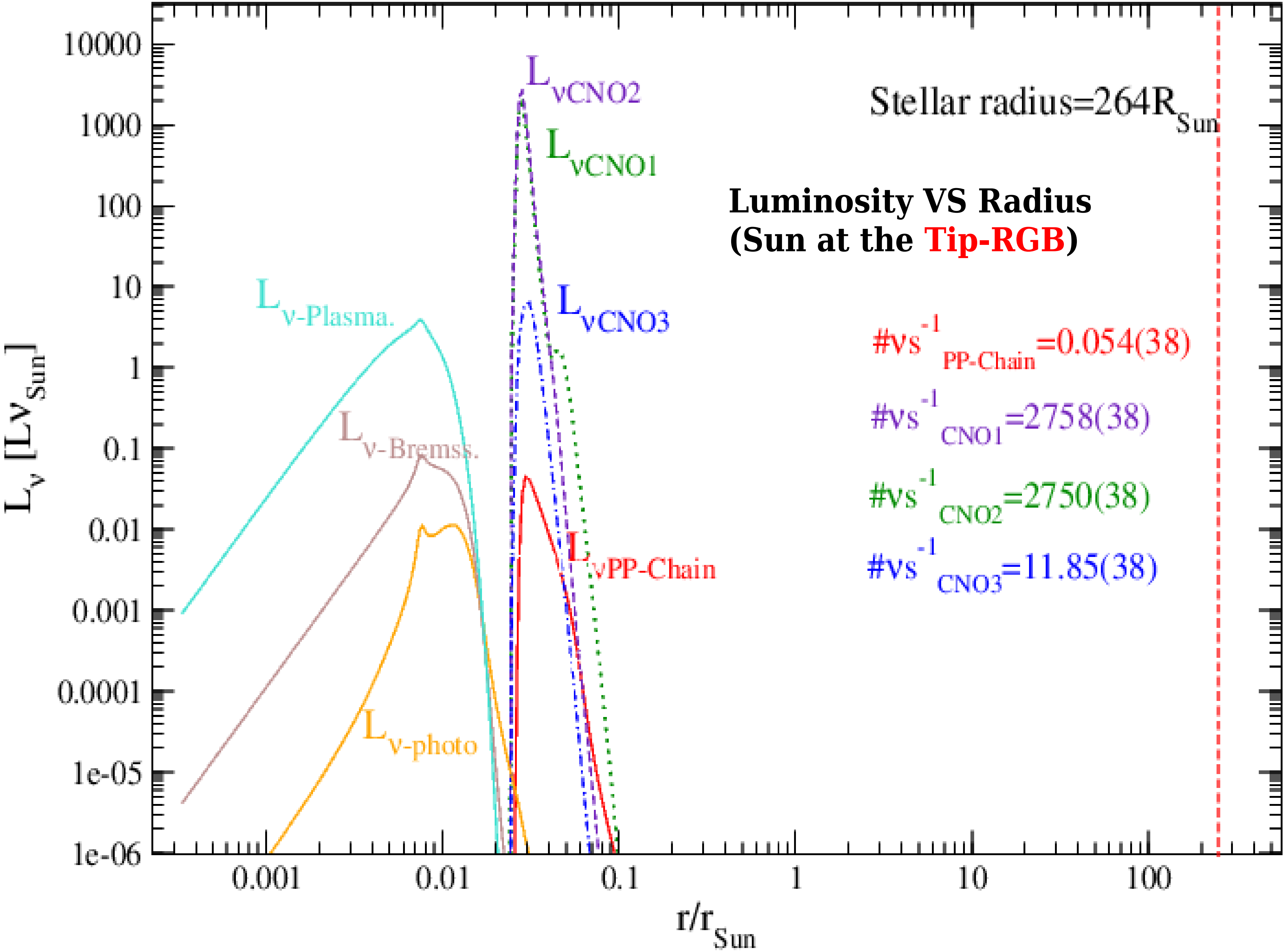
Luminosity VS Radius
(Sun at the Tip-RGB)
Stellar radius=264R_Sun
$L_{\nu CNO2}$
$L_{\nu CNO1}$
$L_{\nu CNO3}$
$L_{\nu\text{-Plasma.}}$
$L_{\nu\text{-Bremss.}}$
$L_{\nu\text{-photo}}$
$L_{\nu PP\text{-Chain}}$
$\#\nu s^{-1}_{PP\text{-Chain}}=0.054(38)$
$\#\nu s^{-1}_{CNO1}=2758(38)$
$\#\nu s^{-1}_{CNO2}=2750(38)$
$\#\nu s^{-1}_{CNO3}=11.85(38)$
$L_\nu\ [L\nu_{Sun}]$
r/r_{Sun}
10000
1000
100
10
1
0.1
0.01
0.001
0.0001
1e-05
1e-06
0.001
0.01
0.1
1
10
100

The effect on enhanced energy losses during the RGB

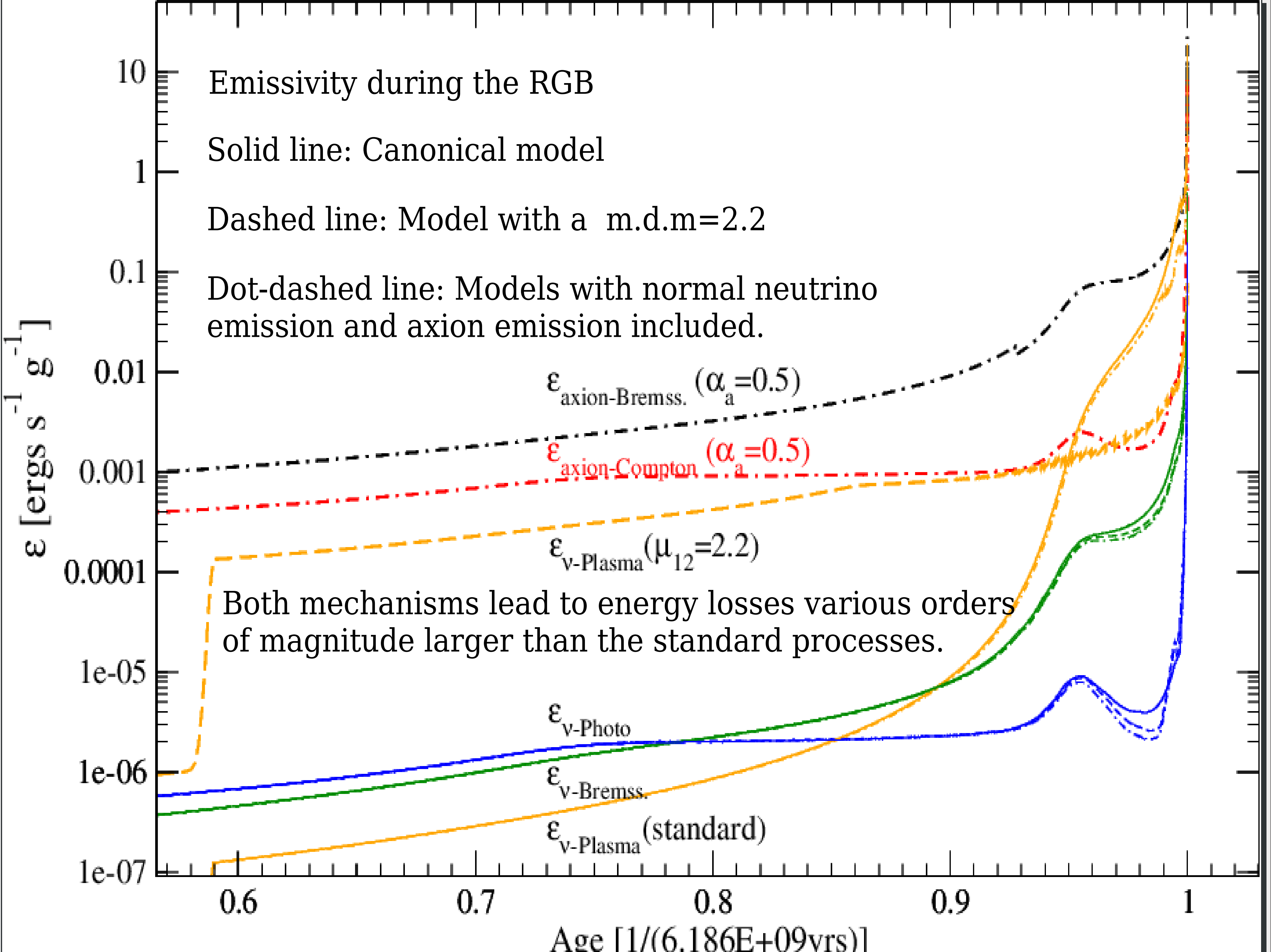

Emissivity during the RGB

Solid line: Canonical model

Dashed line: Model with a m.d.m=2.2

Dot-dashed line: Models with normal neutrino emission and axion emission included.

Both mechanisms lead to energy losses various orders of magnitude larger than the standard processes.

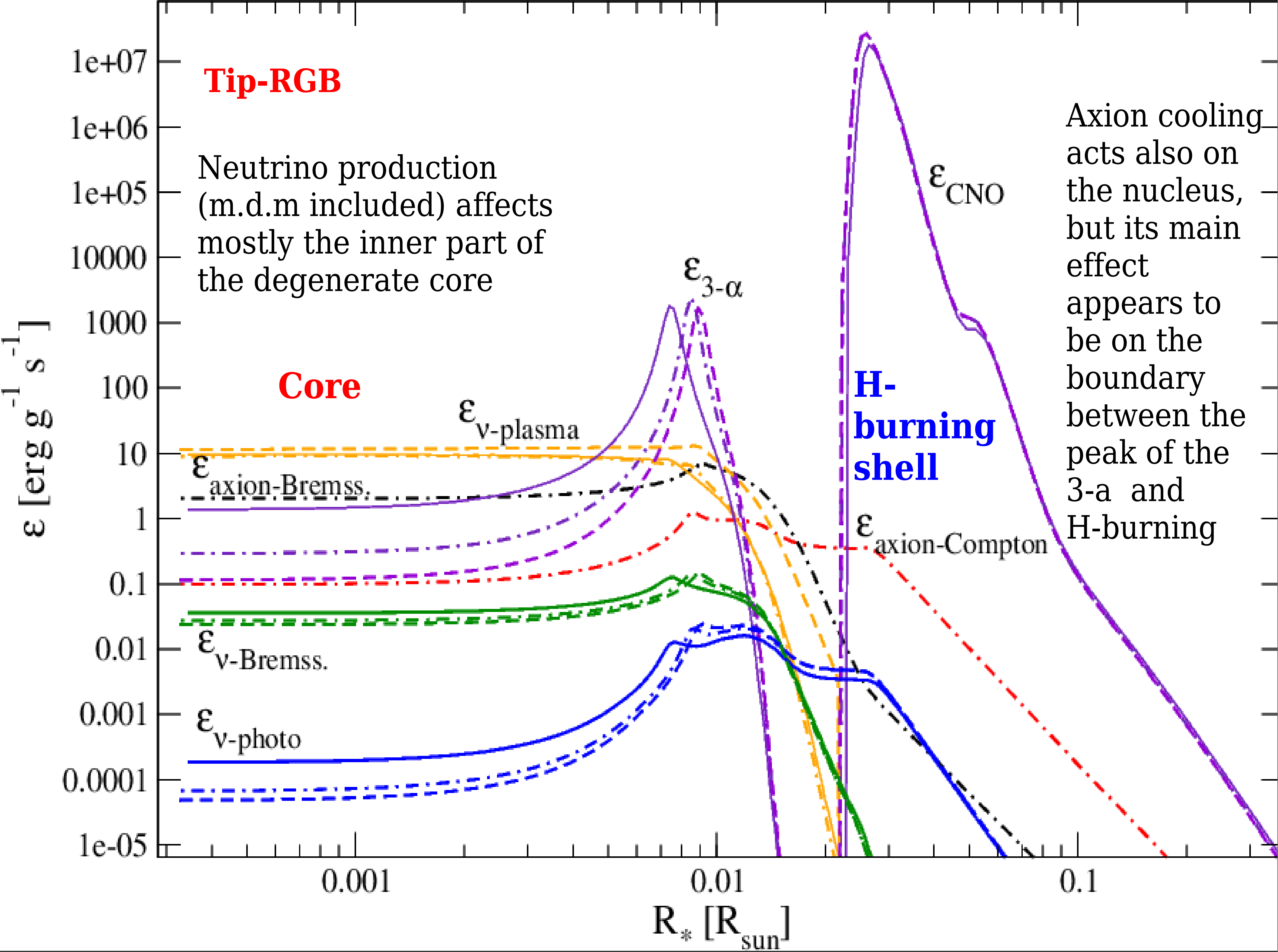

Tip-RGB

Neutrino production (m.d.m included) affects mostly the inner part of the degenerate core

Core

H-burning shell

Axion cooling acts also on the nucleus, but its main effect appears to be on the boundary between the peak of the 3-a and H-burning

The effect of non-standard energy losses on mass-loss

If mass-loss is not reduced, non-standard energy losses suppress stellar evolution

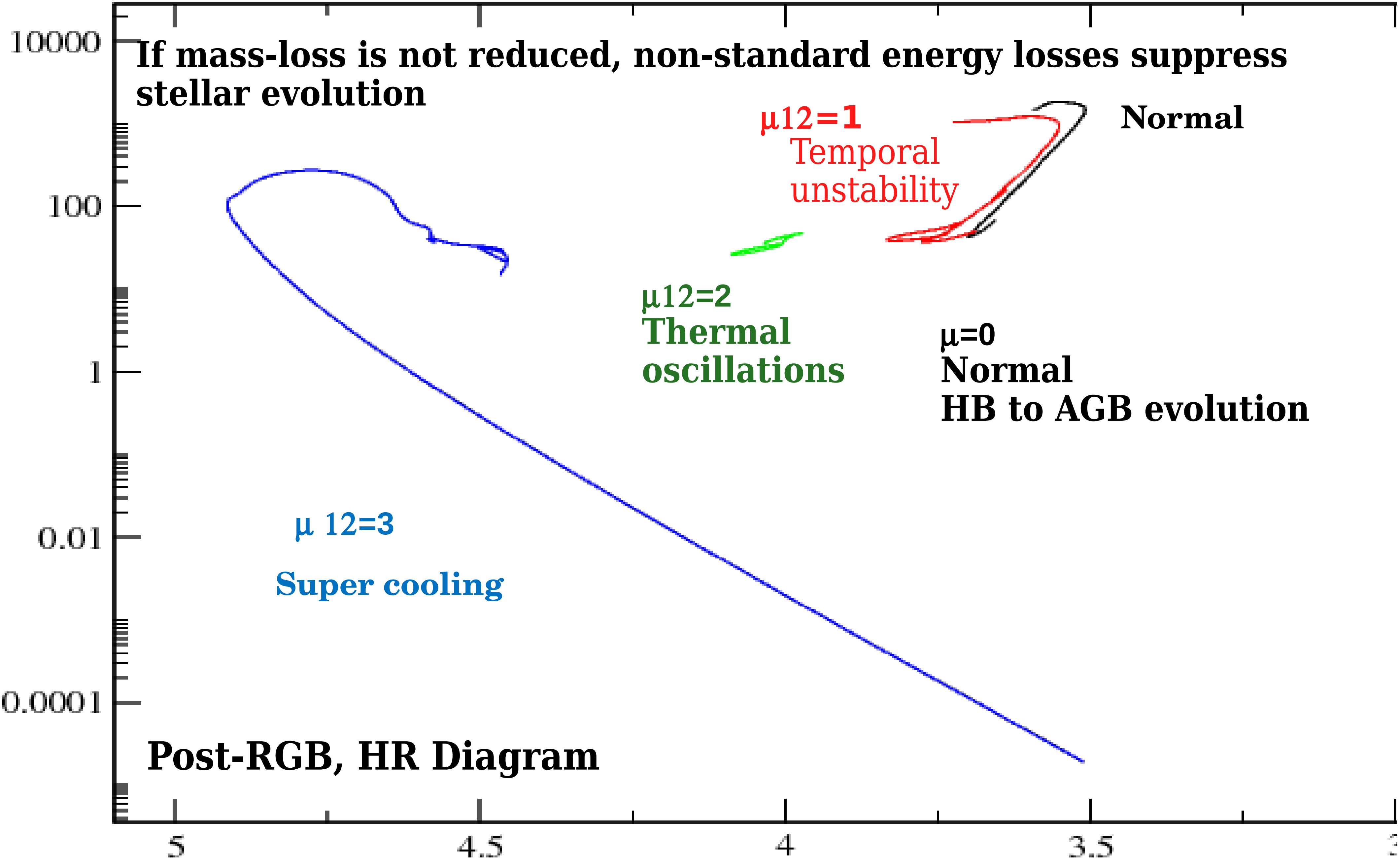

Non-standard energy losses must be as small as to do not stray stellar models from canonical evolution

Depletion of the envelope due enhanced energy losses

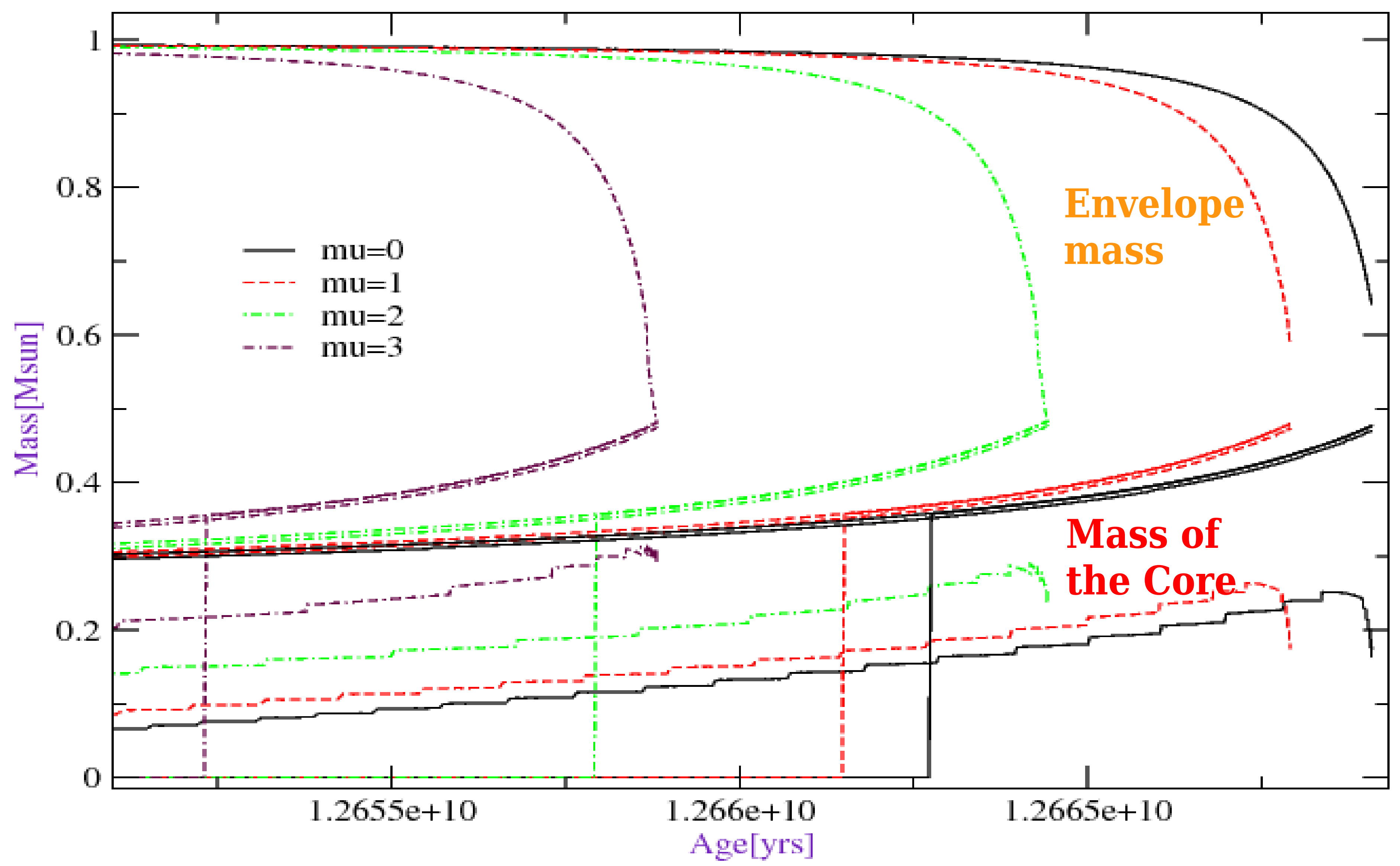

Increasing non-standard energy losses leads to

An artificially accelerated mass-loss rate

Increment on the degeneracy of the Helium core

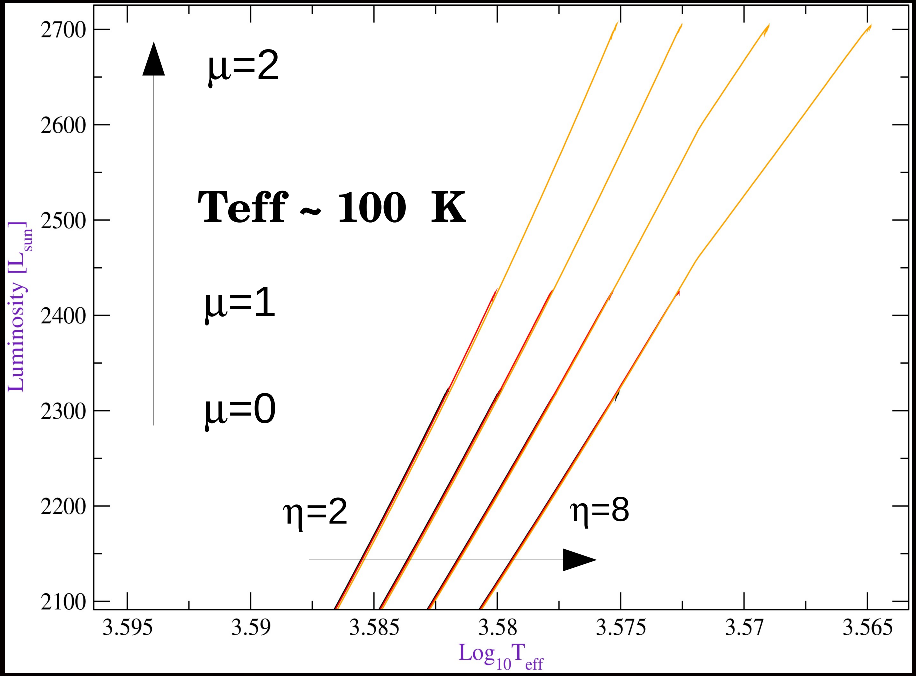
Z=0.001

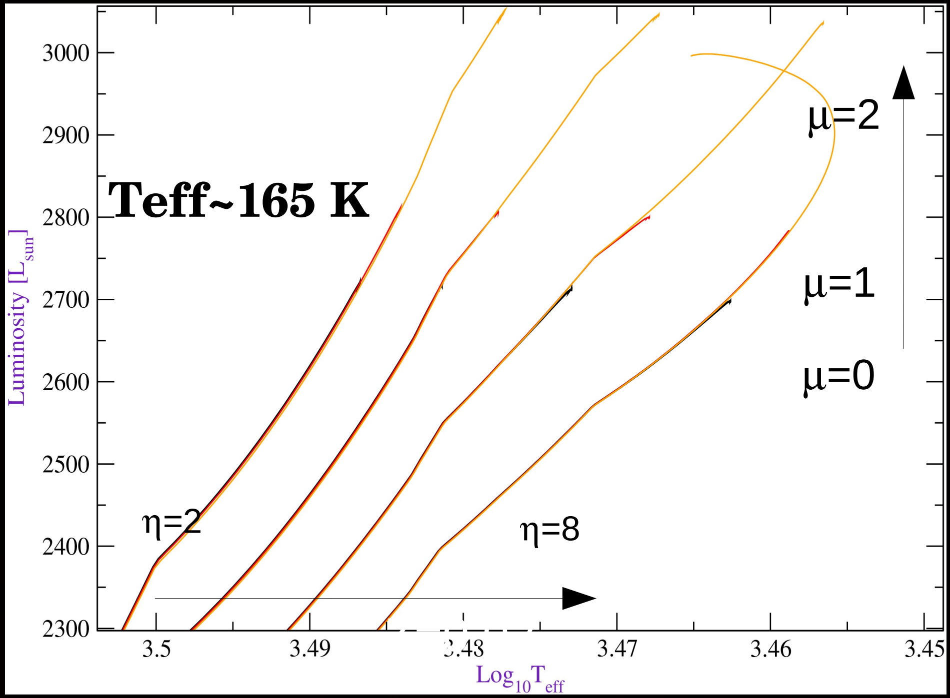
Z=0.01

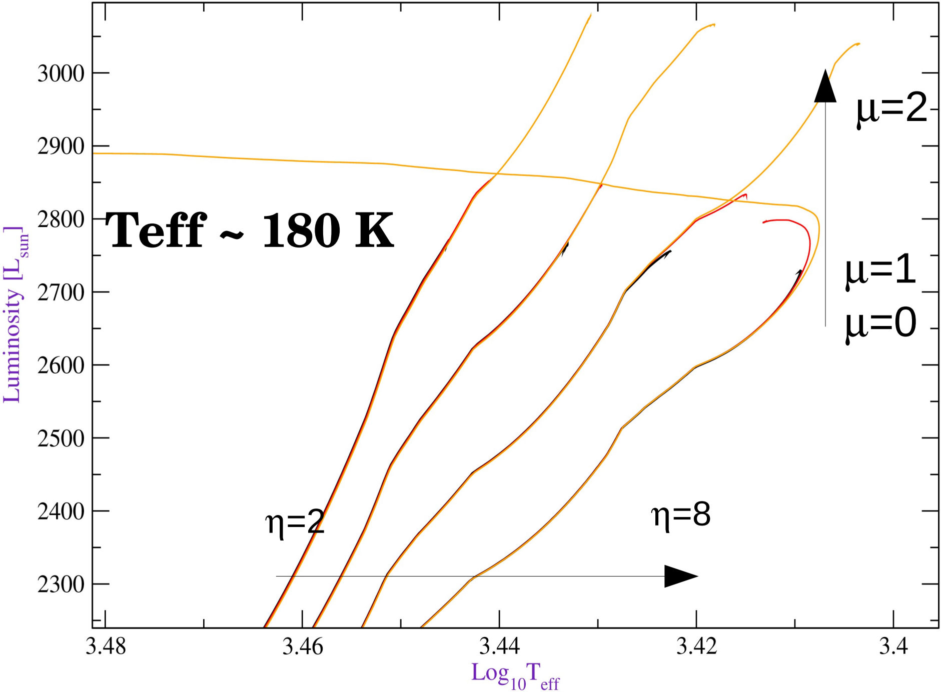
Z=0.02

The tip-RGB luminosity with calibrated mass-loss rate due enhanced energy losses

An specific value for the m.d.m leads to almost the same luminosity level, with only a reduced dependence on the mass-loss rate, initial mass or chemical composition.

Constraints on the neutrino magnetic dipole moment and axion-electron coupling constant by employing NIR data

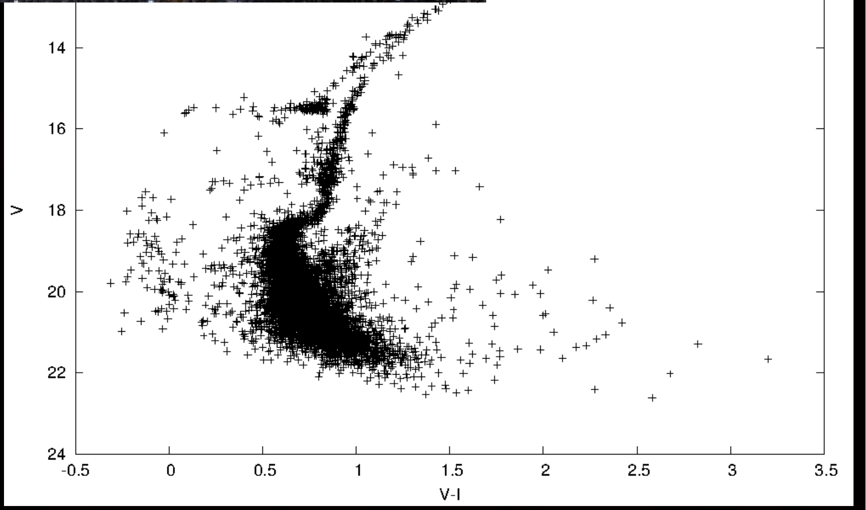

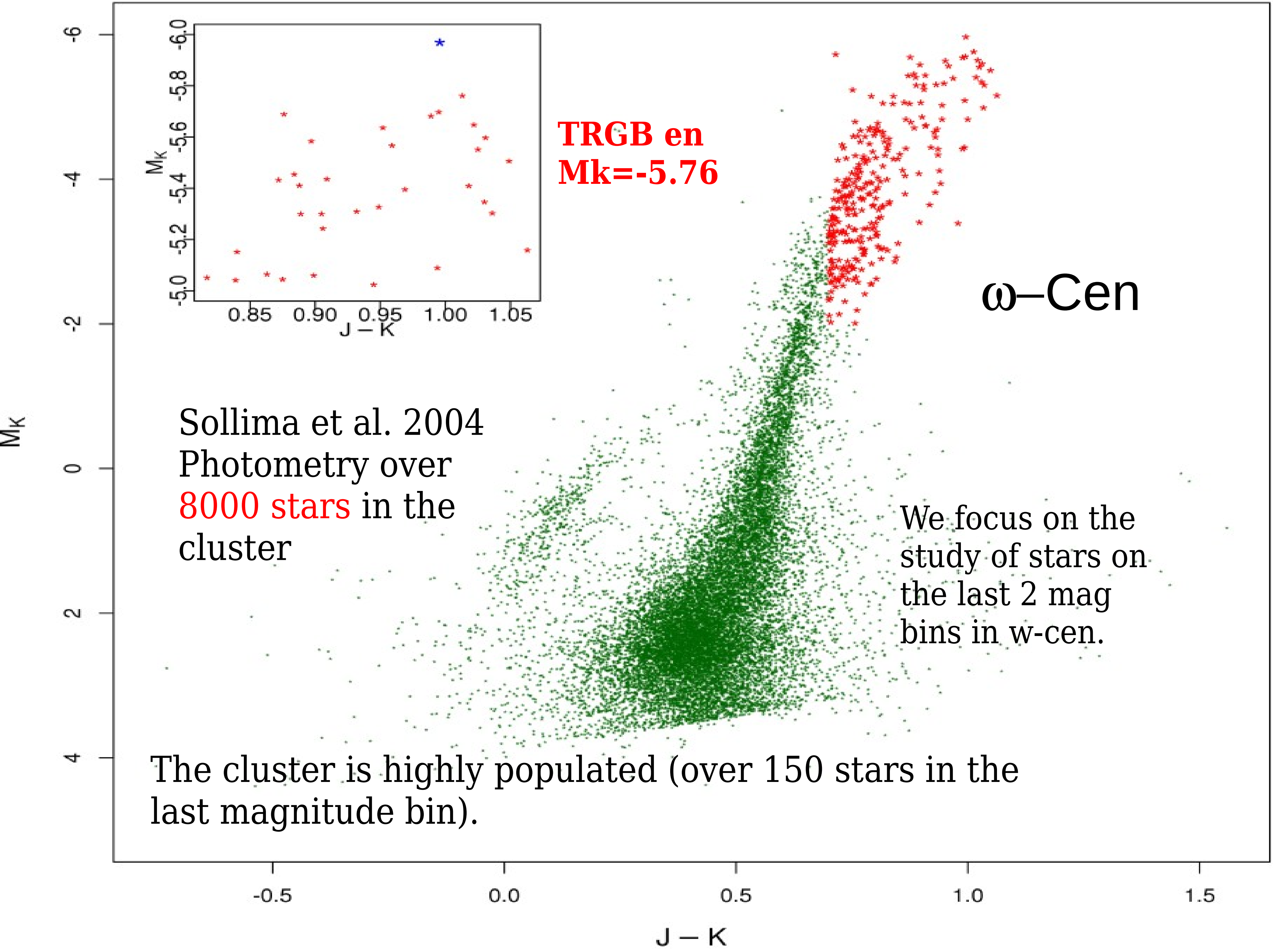

TRGB en Mk=-5.76

ω–Cen

Sollima et al. 2004
Photometry over
8000 stars in the
cluster

We focus on the study of stars on the last 2 mag bins in w-cen.

The cluster is highly populated (over 150 stars in the last magnitude bin).

The highly dense population in Omega-Centauri allows to determine its true tip with an statistical uncertainty of about 0.017 mag. The total uncertainty on the position of the true tip is around 0.16 mag

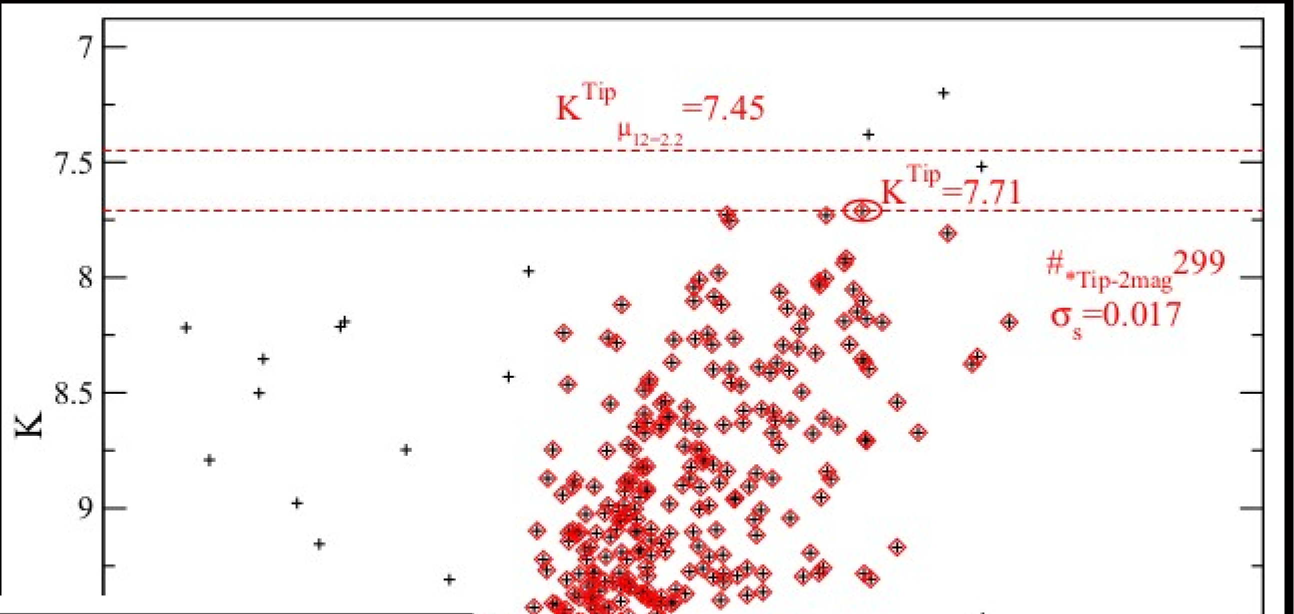

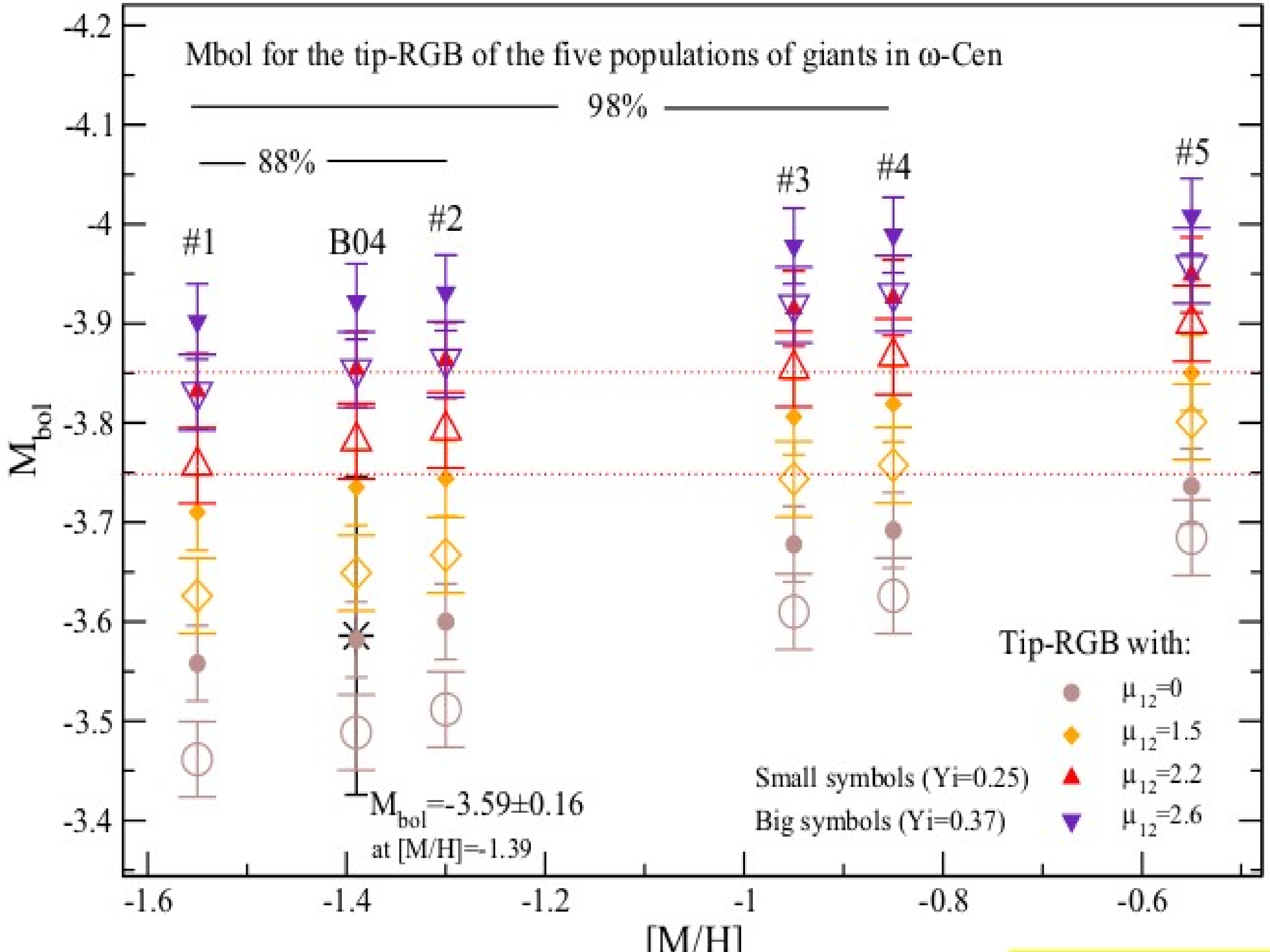

There are five different stellar populations. However, the difference in luminosity due different metallicities is not as big enough as the one due non-standard energy losses

#	Cluster	$[M/H]$	M^{Tip}_{obs}	M^{Tip}_{emp}	M^{Tip}_{0}	$M^{tip}_{\mu_\nu=2.2}$	$M_{\alpha_a=0.}$
1	M92$^{b}_{*}$	-1.95	-3.64±0.26	-3.48	-3.46	-3.76	-3.75
2	M15$^{a}_{*}$	-1.91	-3.55±0.20	-3.49	-3.47	-3.77	-3.75
3	M68^{a}	-1.81	-3.37±0.40	-3.51	-3.53	-3.81	-3.79
4	M30^{a}	-1.71	-3.70±0.35	-3.52	-3.52	-3.82	-3.81
5	M55^{a}	-1.61	-3.71±0.28	-3.54	-3.56	-3.83	-3.82
6	NGC6293$^{d}_{*}$	-1.55	-3.23±0.28	-3.56	-3.56	-3.83	-3.82
7	NGC6255$^{d}_{*}$	-1.43	-3.56±0.26	-3.58	-3.58	-3.85	-3.84
8	NGC6256^{d}	-1.43	-3.56±0.26	-3.58	-3.59	-3.86	-3.84
9	ω-Cen.$^{c}_{*}$	-1.39	-3.59±0.16	-3.59	-3.58	-3.86	-3.86
10	NGC6453^{d}	-1.38	-3.57±0.24	-3.59	-3.60	-3.87	-3.86
11	NGC6522^{d}	-1.33	-3.43±0.26	-3.60	-3.61	-3.87	-3.86
12	Djorg1^{d}	-1.31	-3.68±0.26	-3.60	-3.61	-3.87	-3.86
13	M10^{b}	-1.25	-3.61±0.26	-3.61	-3.65	-3.89	-3.88
14	NGC6273$^{d}_{*}$	-1.21	-3.56±0.26	-3.62	-3.61	-3.87	-3.87
15	NGC6401$^{d}_{*}$	-1.20	-3.42±0.26	-3.62	-3.63	-3.88	-3.87
16	M13^{b}	-1.18	-3.59±0.32	-3.63	-3.66	-3.90	-3.89
17	M3$^{b}_{*}$	-1.16	-3.61±0.24	-3.63	-3.62	-3.88	-3.88
18	NGC6540^{d}	-1.10	-3.56±0.26	-3.64	-3.63	-3.88	-3.87
19	Ter. 9$^{d}_{*}$	-1.01	-3.86±0.26	-3.66	-3.65	-3.90	-3.89
20	NGC362$^{c}_{*}$	-0.99	-2.90±0.21	-3.66	-3.66	-3.91	-3.90
21	NGC6642^{d}	-0.99	-3.66±0.26	-3.66	-3.69	-3.92	-3.96
22	NGC6342^{d}	-0.99	-3.70±0.32	-3.66	-3.75	-3.96	-3.96
23	M4^{a}	-0.94	-3.67±0.22	-3.67	-3.70	-3.92	-3.92
24	HP1^{d}	-0.91	-3.56±0.26	-3.68	-3.69	-3.92	-3.91
25	M5^{b}	-0.90	-3.64±0.28	-3.68	-3.66	-3.93	-3.92
26	NGC6266^{d}	-0.88	-3.47±0.26	-3.68	-3.72	-3.94	-3.93
27	NGC288^{c}	-0.85	-3.80±0.25	-3.69	-3.71	-3.92	-3.95
28	NGC6265^{d}	-0.80	-3.56±0.26	-3.70	-3.68	-3.94	-3.93
29	NGC6638$^{d}_{*}$	-0.78	-3.88±0.35	-3.70	-3.68	-3.93	-3.92
30	M107^{a}	-0.70	-3.57±0.40	-3.71	-3.73	-3.95	-3.94
31	NGC6380$^{d}_{*}$	-0.68	-3.88±0.22	-3.72	-3.70	-3.94	-3.93
32	NGC6569$^{d}_{*}$	-0.66	-3.59±0.26	-3.72	-3.70	-3.95	-3.93
33	Ter. 3$^{d}_{*}$	-0.63	-3.47±0.26	-3.73	-3.74	-3.96	-3.95
34	NGC6539^{d}	-0.60	-3.77±0.26	-3.74	-3.74	-3.96	-3.95
35	47-Tuc$^{a}_{*}$	-0.59	-3.71±0.19	-3.74	-3.70	-3.96	-3.95
36	NGC6637$^{d}_{*}$	-0.57	-3.34±0.31	-3.74	-3.71	-3.95	-3.94
37	NGC6304$^{d}_{*}$	-0.56	-3.59±0.33	-3.74	-3.71	-3.95	-3.94
38	M69^{a}	-0.55	-3.51±0.25	-3.75	-3.75	-3.96	-3.96
39	Ter. 2$^{d}_{*}$	-0.53	-3.81±0.26	-3.75	-3.74	-3.96	-3.95
40	NGC6752^{c}	-0.53	-3.65±0.28	-3.75	-3.66	-3.89	-3.88
41	NGC6441$^{d}_{*}$	-0.52	-3.90±0.20	-3.75	-3.72	-3.94	-3.95
42	NGC6624^{d}	-0.48	-3.85±0.31	-3.76	-3.75	-3.97	-3.97
43	Djorg2$^{d}_{*}$	-0.45	-3.50±0.26	-3.76	-3.76	-3.96	-3.97

We took 50 globular clusters form the largest homogeneous NIR-data base up to date (Valenti, Ferraro & Origlia)

We selected those custers with:

the largest number of stars on the last 2-mag bins

with well defined RGB's

Non obvious multiple stellar populations

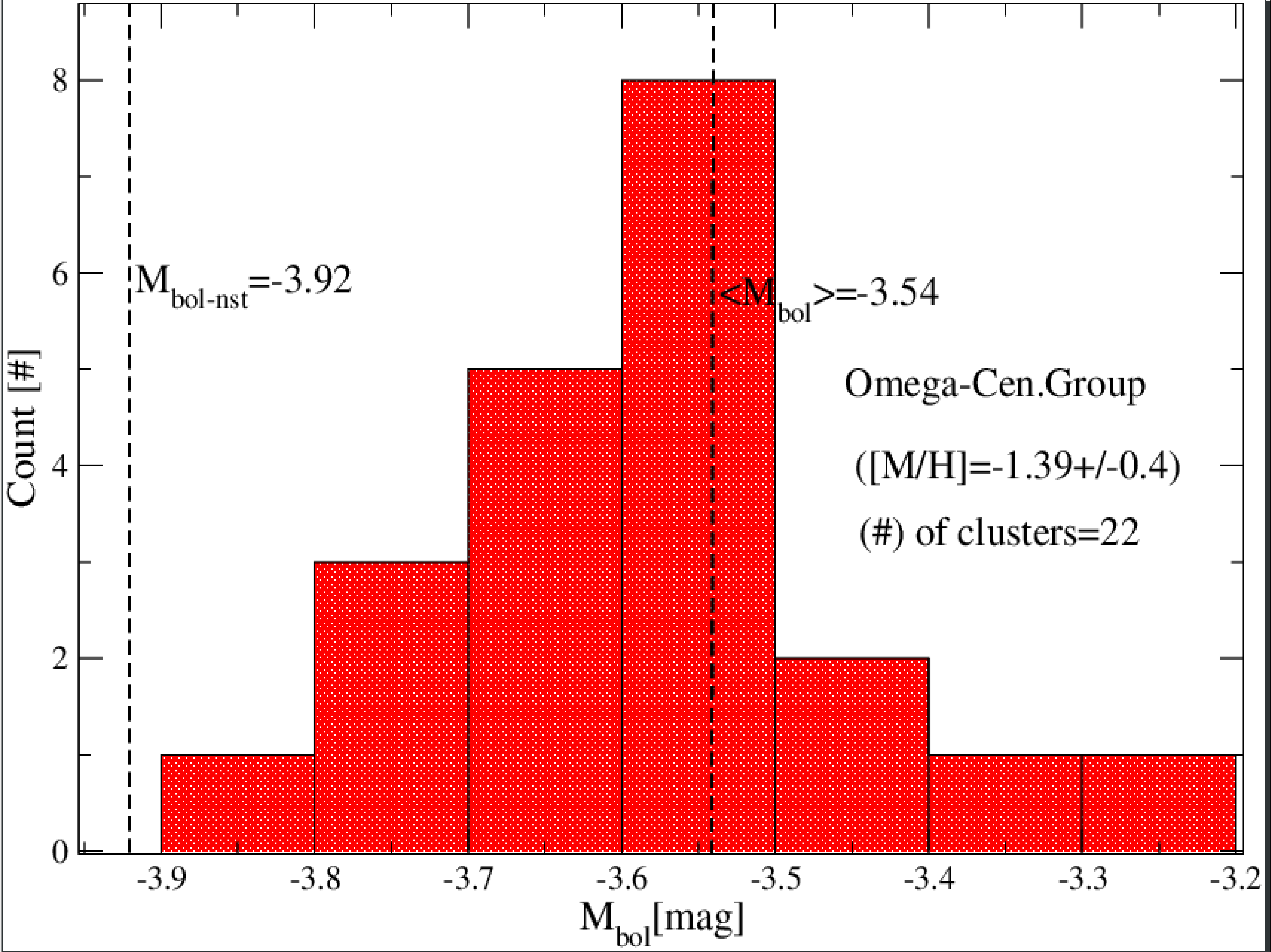
Count [#]
0
2
4
6
8
-3.9
-3.8
-3.7
-3.6
-3.5
-3.4
-3.3
-3.2
M_bol[mag]
M_bol-nst=-3.92
<M_bol>=-3.54
Omega-Cen.Group
([M/H]=-1.39+/-0.4)
(#) of clusters=22

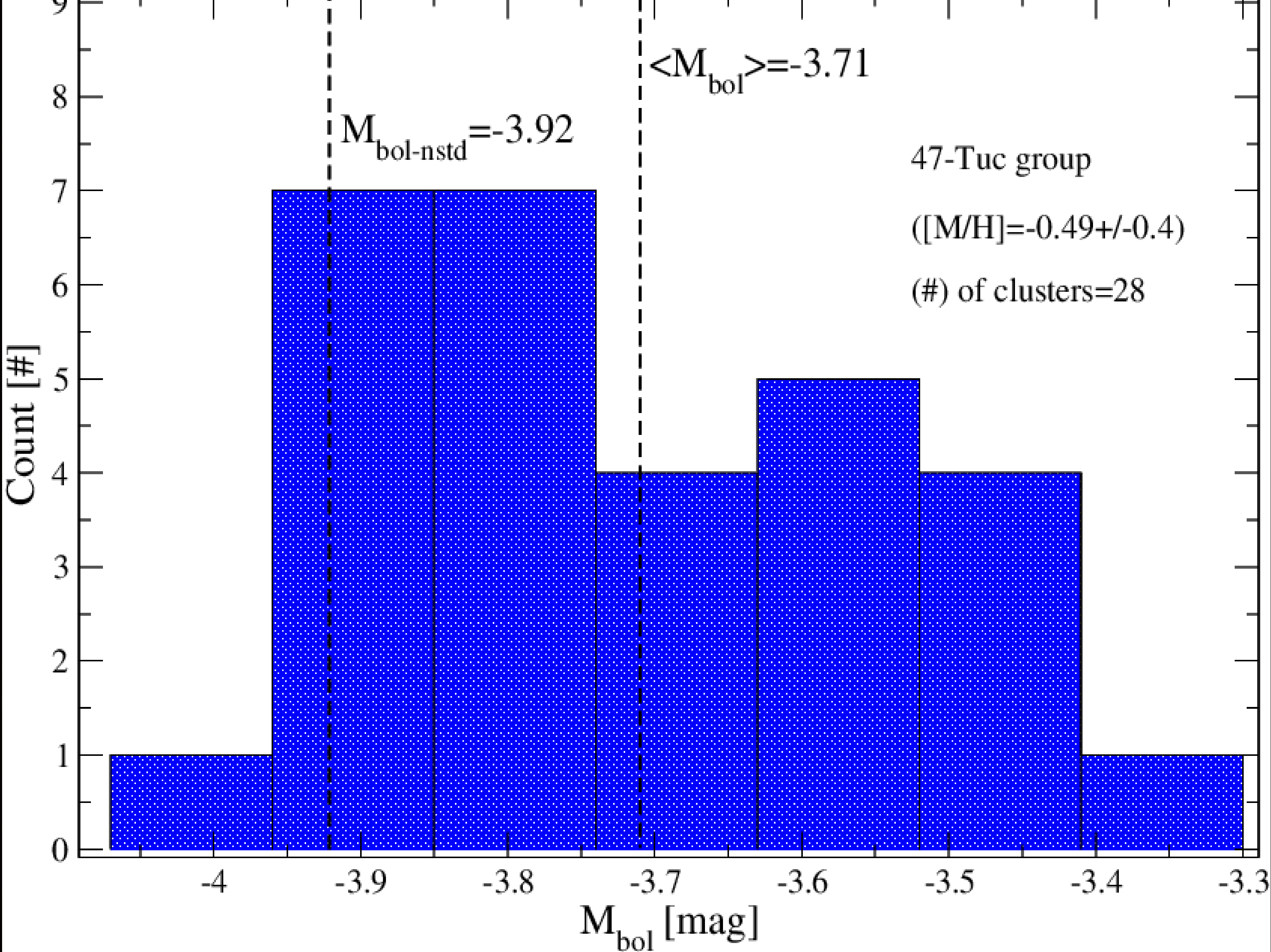
$\langle M_{bol} \rangle = -3.71$
$M_{bol\text{-}nstd} = -3.92$
47-Tuc group
([M/H]=-0.49+/-0.4)
(#) of clusters=28
Count [#]
0
1
2
3
4
5
6
7
8
-4
-3.9
-3.8
-3.7
-3.6
-3.5
-3.4
M_{bol} [mag]

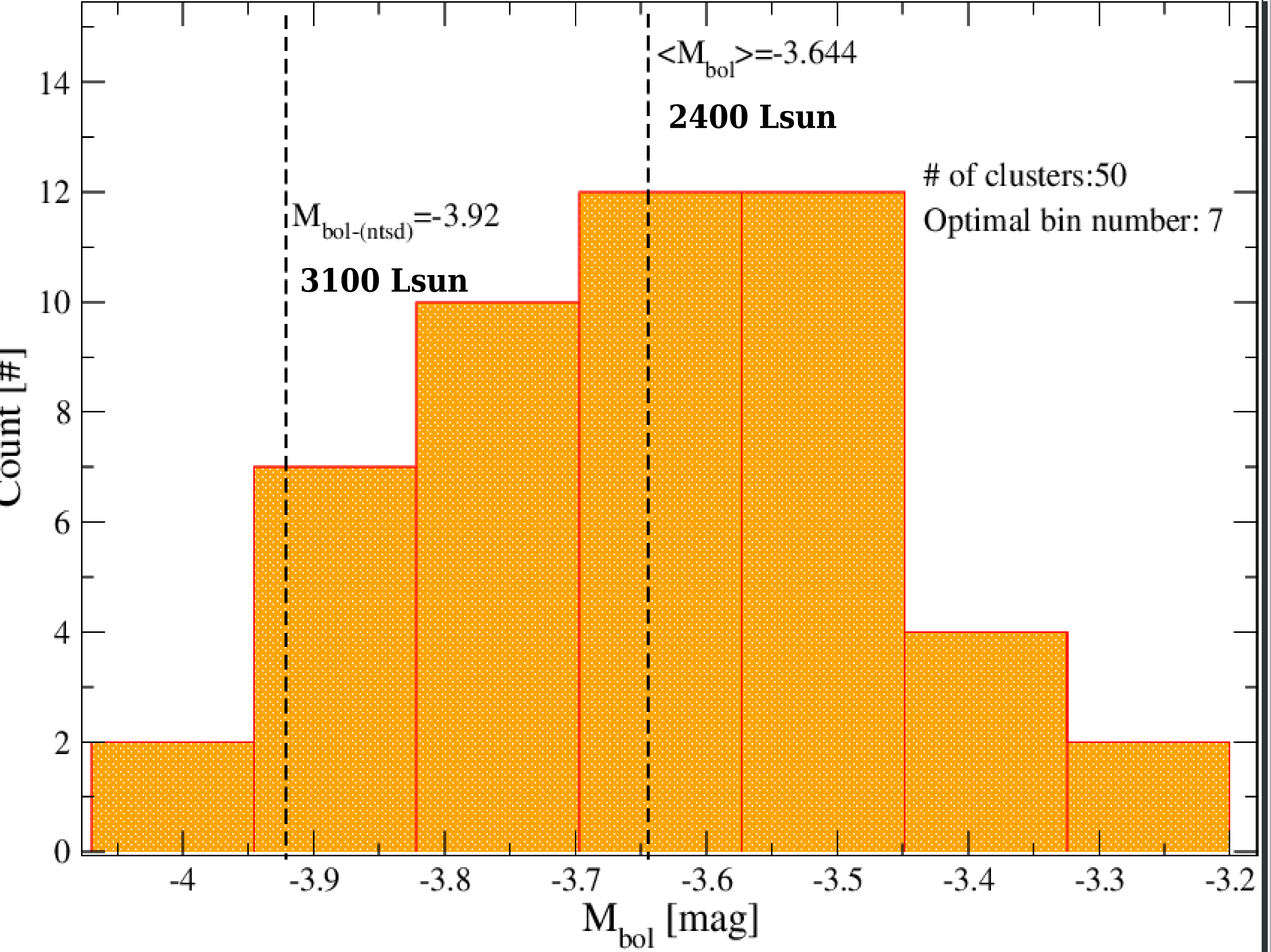

<M_bol>=-3.644
2400 Lsun
M_bol-(ntsd)=-3.92
3100 Lsun
# of clusters:50
Optimal bin number: 7
Count [#]
0
2
4
6
8
10
12
14
-4
-3.9
-3.8
-3.7
-3.6
-3.5
-3.4
-3.3
-3.2
M_bol [mag]

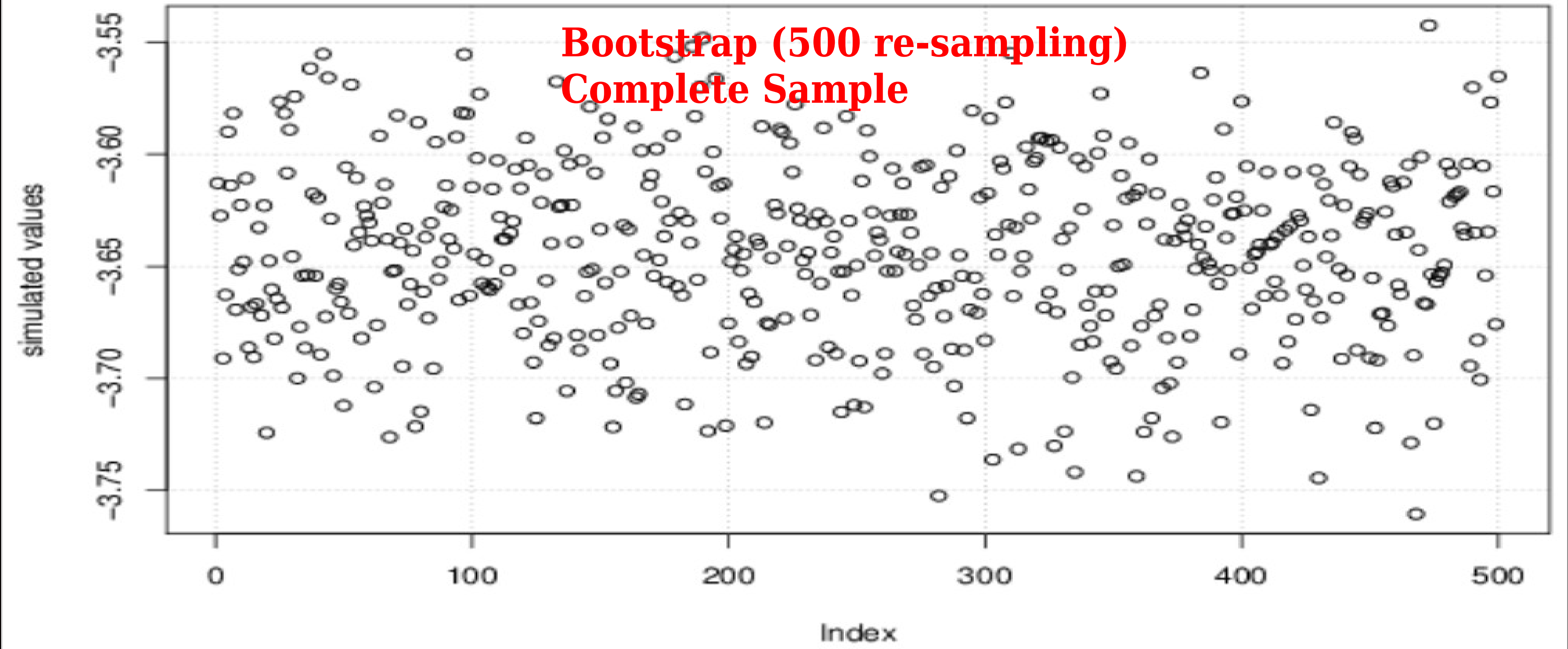

Bootstrap (500 re-sampling)
Complete Sample

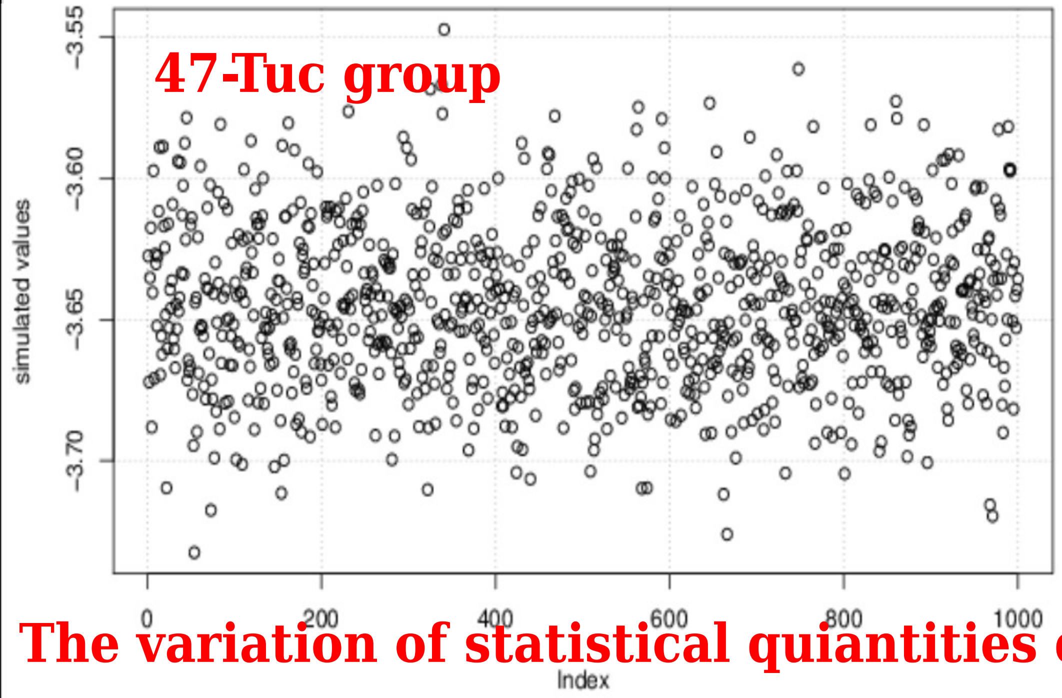

47-Tuc group

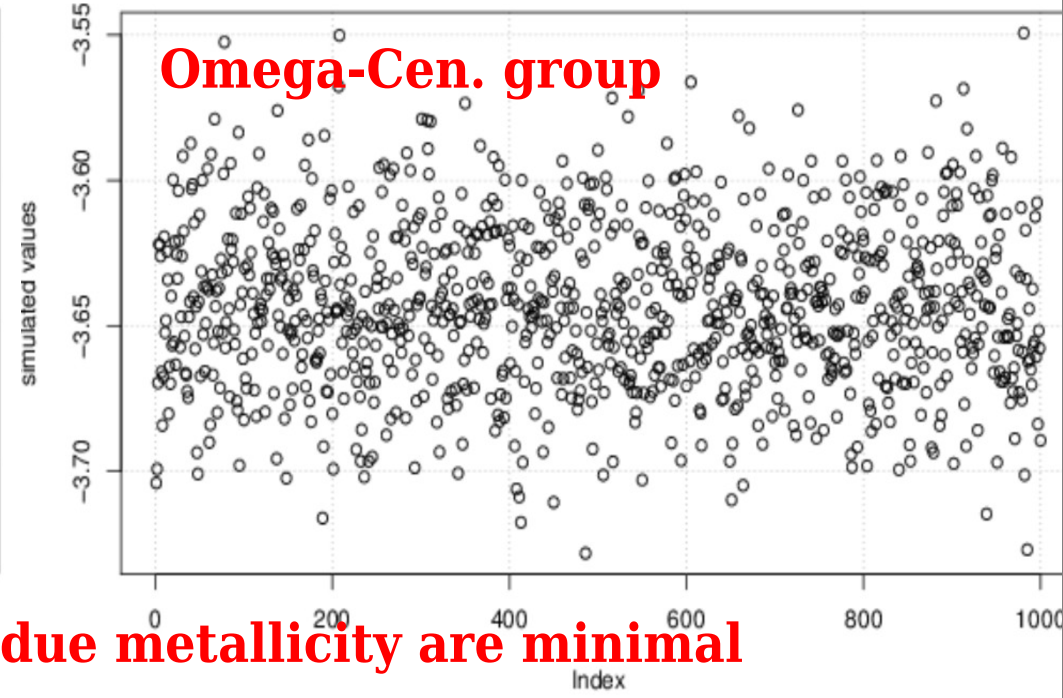

Omega-Cen. group

The variation of statistical quiantities due metallicity are minimal

Mean bolometric magnitude of our sample: $\left\langle M^{Tip}_{obs} \right\rangle = -3.65,\ \sigma_{obs} = 0.17$

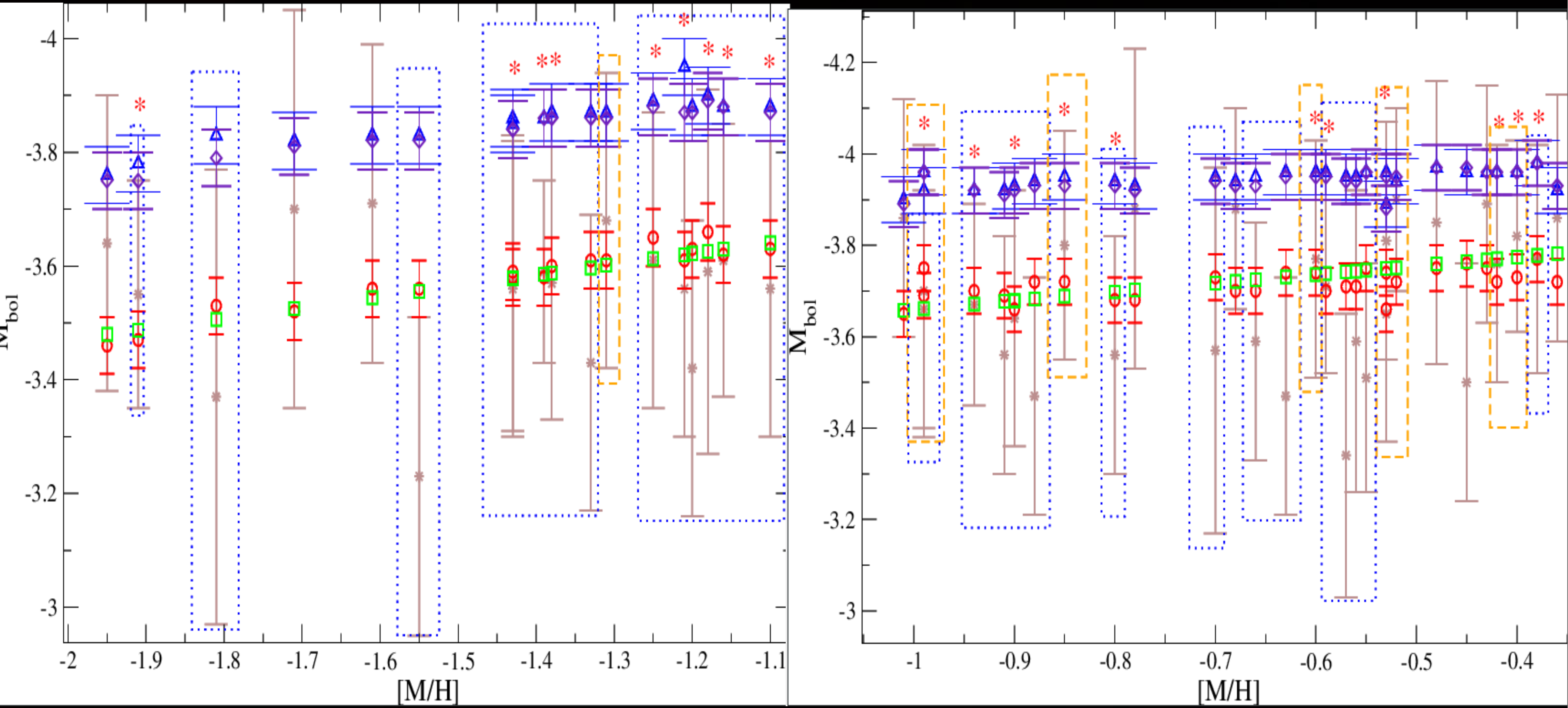

According the sample data we can put the constraints

$$\mu_\nu \leq 2.2 \times 10^{-12} \mu_B \qquad \alpha_a \sim 0.5 \times 10^{-26}$$

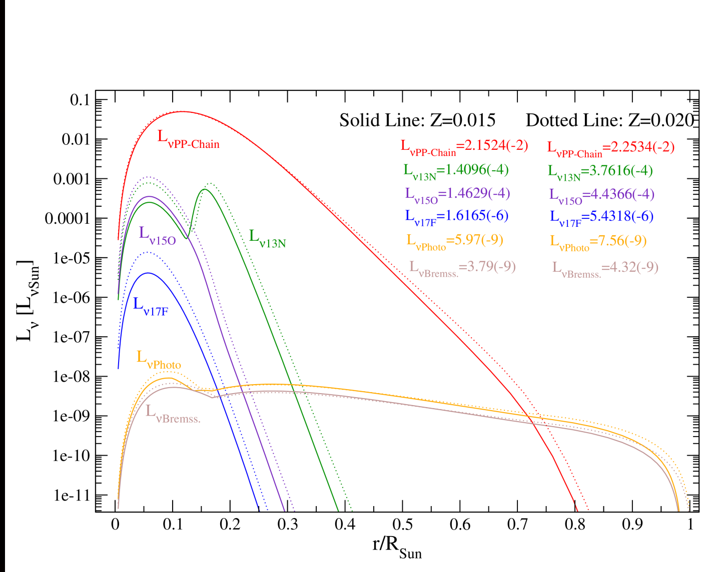

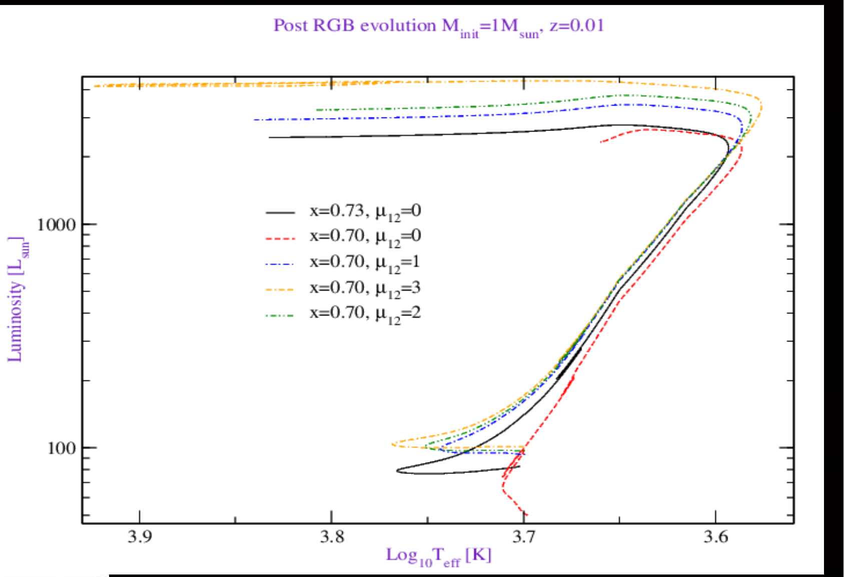

Additional results

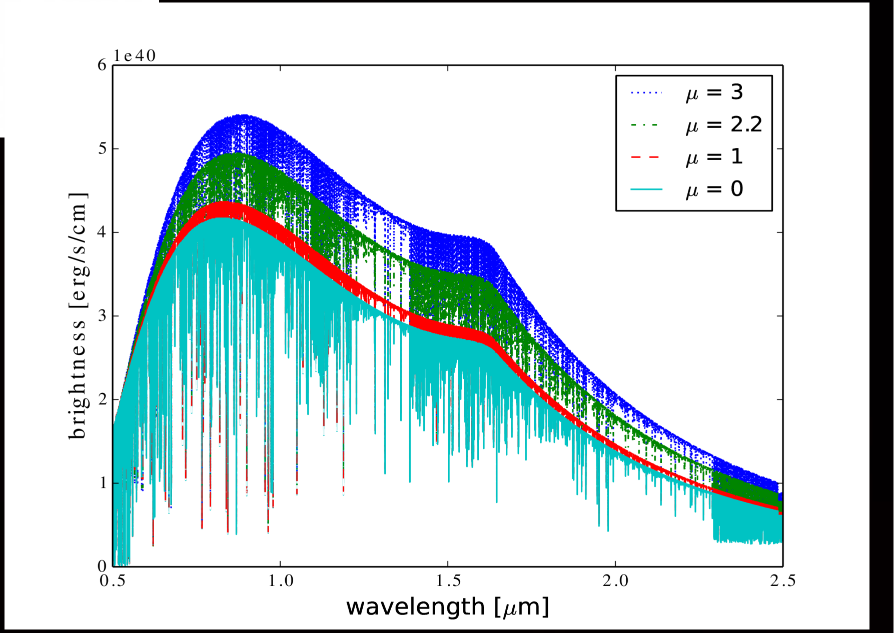

Stellar evolution $M_{init}=1M_{sun}$, $Z=0.01$

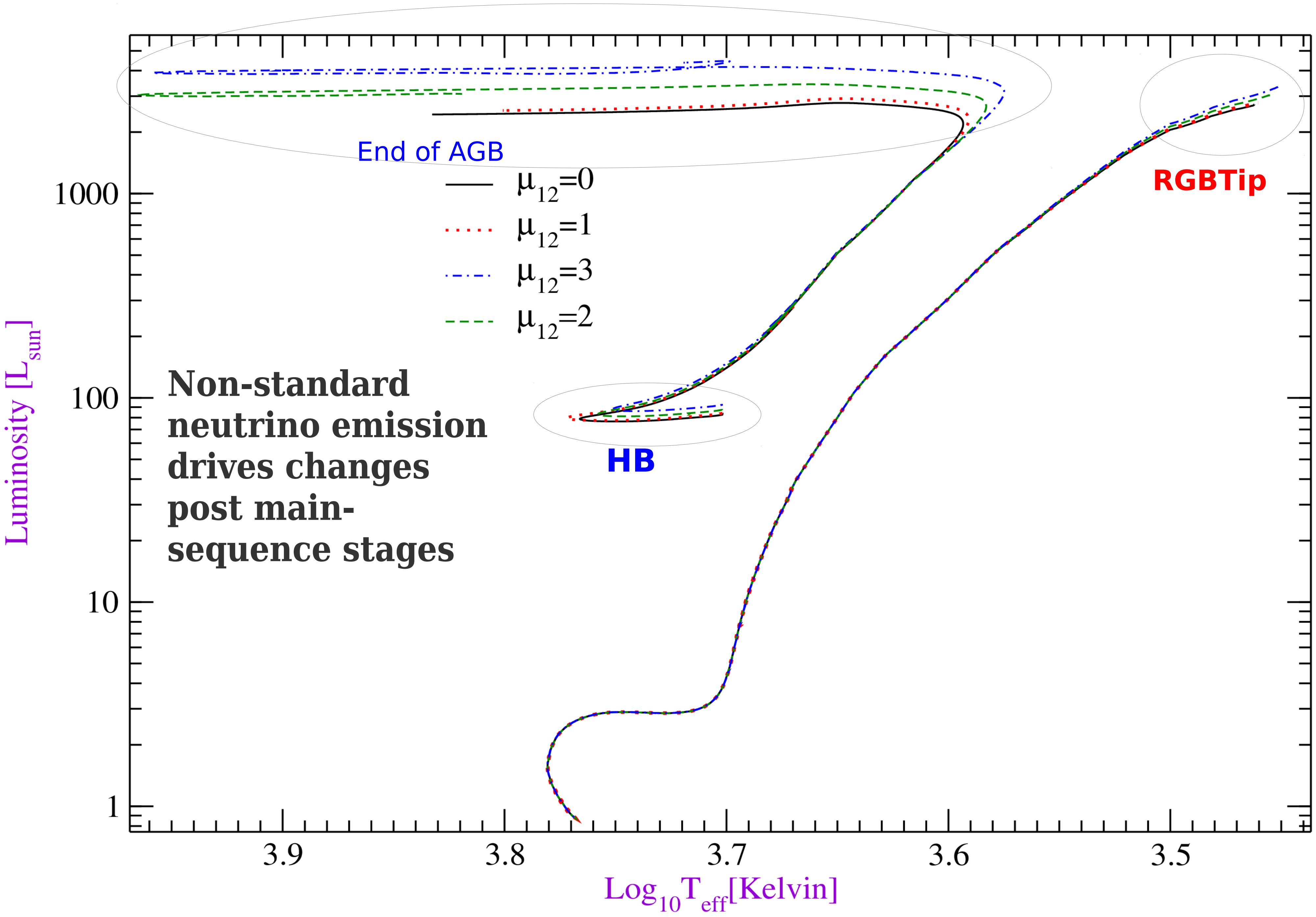

Non-standard neutrino emission drives changes post main-sequence stages

Changes on the HB due more massive cores

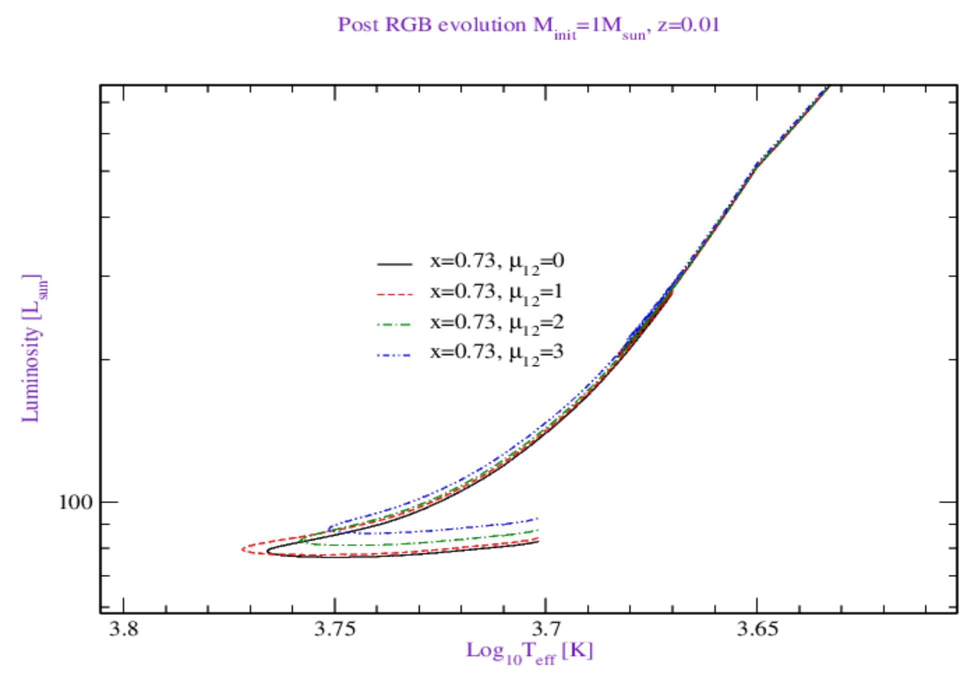

Non-standard energy losses accelerate Helium burning. This changes:

The HB length

The position of the Turn-off point for Helium

Further work

Non-standard energy losses could allow stellar models with an Helium over abundance of about DY=0.03 to mimic the same HB length as the canonical models

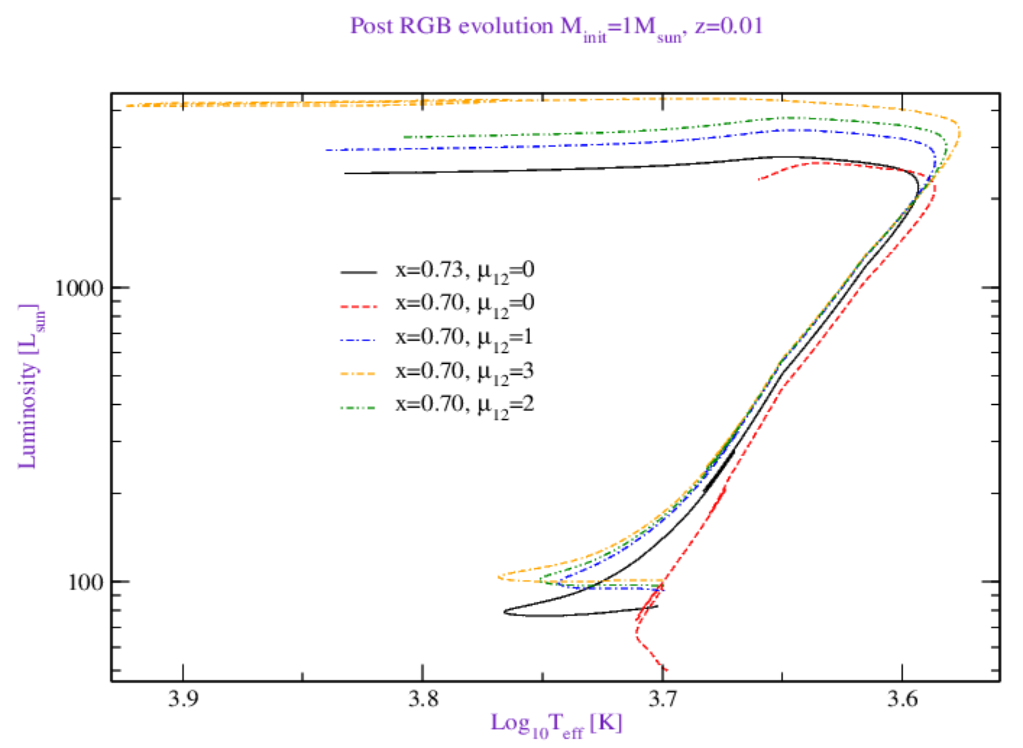

Synthetic spectra with the PHOENIX Code

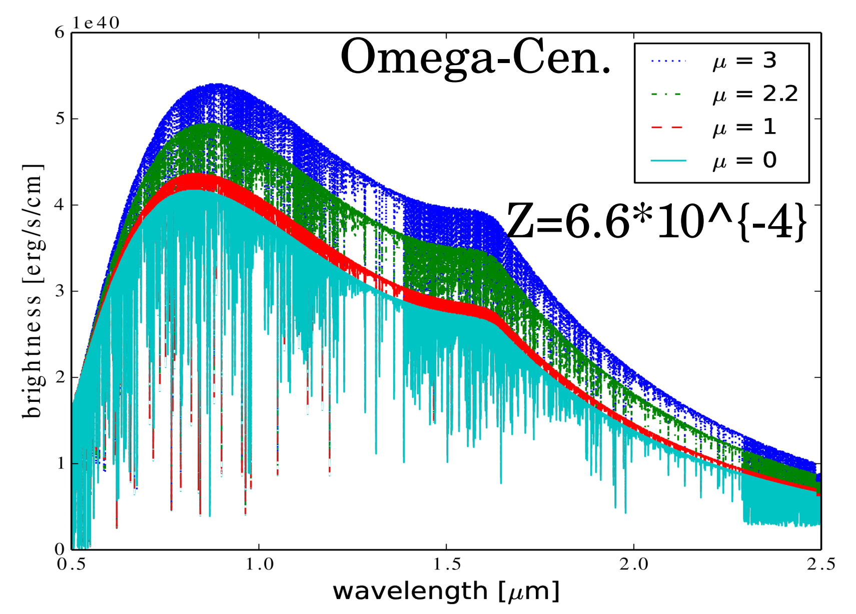

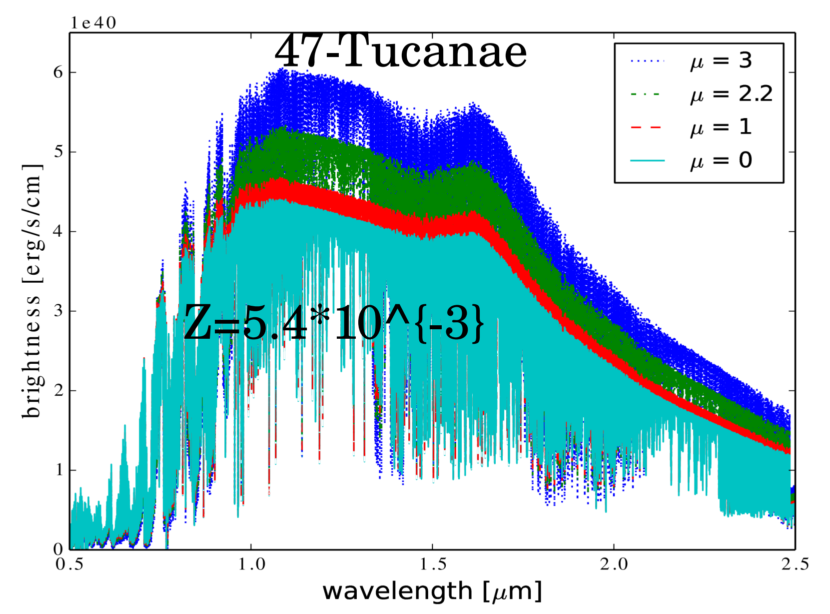

The enhancement in flux is different for multiple bands on the NIR- spectrum

Causes: Lower surface gravity

Increment on the flux

Line blanketing affects the spectra of more metallic stars

Optimal observations of the enhanced flux due non-standard neutrino emission on the H and J bands

Acknowledgments to my advisers:

Dr. Klaus-Peter Schroeder

Astronomy Department,
Guanajuato University,
México

Dr. Kai Zuber

Physics Department, IKTP,
University of Dresden,
Germany

Dr. Dennis Jack

Astronomy Department,
Guanajuato University,
México

Gracias por su atención!